

Pushing the Frontier of Audiovisual Perception with Large-Scale Multimodal Correspondence Learning

Apoorv Vyas*, Heng-Jui Chang*, Cheng-Fu Yang*, Po-Yao Huang*, Luya Gao*, Julius Richter*, Sanyuan Chen†, Matt Le†, Piotr Dollár‡, Christoph Feichtenhofer‡, Ann Lee‡, Wei-Ning Hsu‡

Meta Superintelligence Labs

*Core contributors (random order from second author onward), †Contributors (random order), ‡Project leads (random order)

We introduce Perception Encoder Audiovisual, PE_{AV} , a new family of encoders for audio and video understanding trained with scaled contrastive learning. Built on PE [8], PE_{AV} makes several key contributions to extend representations to audio, and natively support joint embeddings across audio-video, audio-text, and video-text modalities. PE_{AV} ’s unified cross-modal embeddings enable novel tasks such as speech retrieval, and set a new state of the art across standard audio and video benchmarks. We unlock this by building a strong audiovisual data engine that synthesizes high-quality captions for $\mathcal{O}(100\text{M})$ audio-video pairs, enabling large-scale supervision consistent across modalities. Our audio data includes speech, music, and general sound effects—avoiding single-domain limitations common in prior work. We exploit ten pairwise contrastive objectives, showing that scaling cross-modality and caption-type pairs strengthens alignment and improves zero-shot performance. We further develop $\text{PE}_{\text{A-Frame}}$ by fine-tuning PE_{AV} with frame-level contrastive objectives, enabling fine-grained audio-frame-to-text alignment for tasks such as sound event detection.

Code:

https://github.com/facebookresearch/perception_models

<https://huggingface.co/collections/facebook/perception-encoder-audio-visual>



1 Introduction

Vision, audio, and language are fundamental modalities in human perception. Audio often provides complementary or disambiguating cues for visually subtle or ambiguous actions (*e.g.*, distinguishing “speaking” vs. “whispering”). Audio can also carry distinct visual concepts, such as an ambulance siren warning us of an emergency vehicle before it comes into sight while driving. Perceptual and neuroscience studies further suggest that audio and visual signals are tightly coupled in the brain—as *e.g.* illustrated by the McGurk effect [59], where listening to an audio clip (*e.g.*, sounding “ba-ba”) while watching fabricated lip movements (indicating “va-va”) changes the perceived sound (from “ba-ba” to “va-va”).

Multimodal correspondences can therefore be used to learn *semantic* representations that align text, audio, and vision. Consider, *e.g.*, that an ambulance vehicle representation could be learned from any combination of video of an ambulance, its distinctive sound, or a text description. Such representations can, in turn, be directly used for downstream applications such as classification and retrieval.

Contrastive models demonstrate strong performance in aligning individual modalities (*e.g.*, images or audio) to text [73, 96, 100, 104]. Recent works like ImageBind [33], LanguageBind [111], and InternVideo2 [94] connect more modalities via an “anchor” modality. However, imbalanced scale and diversity across modality pairs continue to limit performance. While there has been large progress in vision-language learning with CLIP [73] and its follow-up works, the audio-video domain remains underrepresented and lags behind in performance.

In this work, we build Perception Encoder Audiovisual (PE_{AV}), a family of audio-visual-text aligned encoders trained with a simple contrastive objective across modalities. Our approach is centered on the *scale* and *quality* of synthetic data, data types, loss pairs, and model size.

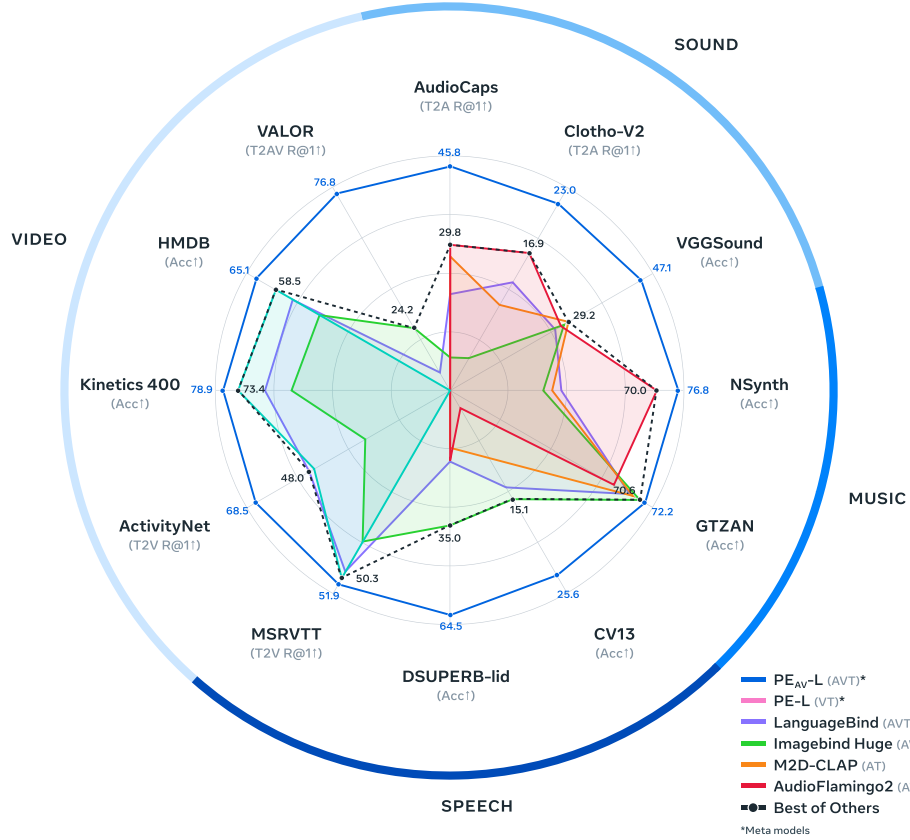


Figure 1 Perception Encoder Audiovisual (PE_{AV}) is a family of audio-video-text (AVT) encoders. By scaling coverage of contrastive learning, model size, and training with synthetically aligned video-audio-text pairs across diverse domains, PE_{AV} achieves state-of-the-art performance on a wide range of zero-shot sound, music, speech, and video classification and retrieval tasks.

We build a robust audiovisual data engine that generates high-quality synthetic captions at scale. We start by using an LLM to combine information from multiple weak audio captioning models along with their confidence scores, and video captions to produce captions for audio, visual, and audio-visual information in *unlabeled* video clips. We train an initial version of PE_{AV} on these synthetic labels. This PE_{AV} is then used with an LLM decoder to generate refined audiovisual captions. Our two-stage data engine yields reliable captions for $\mathcal{O}(100M)$ audio-video pairs, dramatically expanding beyond existing data while producing a corpus well balanced across modalities.

In the modeling part, we scale the contrastive objective to encompass up to *ten* cross-modal pairs among video, audio, and diverse text captions. Expanding the coverage of modality pairs consistently enhances alignment and enables joint embeddings for audio-text, video-text, and audio-video. For the model architecture, we employ separate audio and vision towers, followed by a joint audio-visual encoder. We use PE [8] as a video frame encoder, followed by a stack of temporal transformer blocks to capture temporal dynamics, as an efficient vision architecture for encoding videos.

We train PE_{AV}'s audio encoder at three scales (0.1-1.1 billion parameters) and see consistent gains in zero-shot retrieval and classification of video, sound, music, and speech. As shown in Fig. 1, PE_{AV}L sets a new state-of-the-art (SoTA) performance on multiple audio-video benchmarks compared to recent audio-text [27, 32, 67, 96], and audio-video-text models [33, 111]. Notably, on AudioCaps, text-to-audio improves from 35.4 R@1 to 45.8 R@1; and on VGGSound, classification accuracy improves from 36.0 to 47.1. PE_{AV} is the only model to enable speech retrieval (85.6 while others are near 0). On video benchmarks, PE_{AV}L improves ActivityNet text-to-video retrieval from 60.4 R@1 to 66.5 R@1, and video classification on Kinetics-400 from 76.9 to 78.9 accuracy, surpassing models 2–4× larger [8, 94].

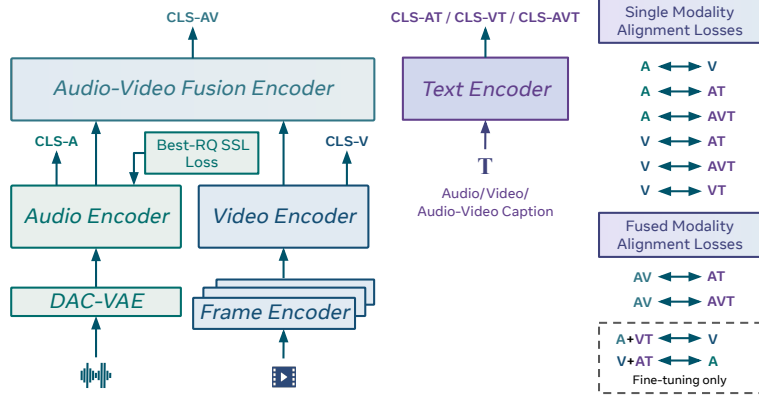


Figure 2 **Perception Encoder-AudioVisual (PE_{AV})** is composed of an audio encoder, a frame encoder, video encoder, audio-video fusion encoder and a text encoder. For audio we use DAC-VAE to encode raw audio waveforms. For video we directly encode raw RGB frames. We use eight contrastive loss to associate embeddings of eight types of multimodal pairs. We use two extra pairs during fine-tuning stage adding to a total of ten loss pairs.

In summary, PE_{AV}’s main contributions are:

- **A strong multimodal data engine.** Our audiovisual data engine produces high-quality, diverse synthetic captions at scale that outperform real captions in synthetic *vs.* real comparisons. Their complementary nature further boosts accuracy when combined.
- **A broad learning paradigm.** Ten training objectives improve alignment across modalities and data types.
- **Unprecedented domain coverage.** Our audio encoder supports speech, music, and general sound-effects, unlike prior audio models that specialize in a single domain.
- **Unified cross-modal embeddings:** Beyond separate audio, video, and text embeddings, PE_{AV} learns to jointly encode audio-video, audio-text, and video-text at scale, achieving SoTA zero-shot performance on video classification and retrieval, sound and music tasks, and speech benchmarks. We release our models and code to support reproducibility and future research and applications.

Finally, we introduce *Perception Encoder Audio-Frame* (PE_{A-Frame}), which fine-tunes PE_{AV} using a frame-level contrastive loss. Moving beyond utterance-level, PE_{AV} enables fine-grained frame-level audio-to-text alignments. PE_{A-Frame} performs strongly across open- and closed-vocabulary sound event detection (SED), achieving top results in identifying target-sound events across benchmarks. It yields the best performance on all open-vocabulary tests and real-world benchmark such as the closed-set DESED [89].

2 Perception Encoder for Audio and Video

As shown in Fig. 2, PE_{AV} consists of a text encoder, a video-frame encoder, a video encoder, an audio feature extractor, an audio encoder, and an audio-video fusion encoder. PE_{AV} is trained using contrastive objectives on videos with synthetic captions $\mathcal{O}(100M)$ and a few real datasets $\mathcal{O}(5M)$. The synthetic audio, visual, and audio-visual captions are powered by an audiovisual data engine described next.

2.1 PE_{AV} Data Engine

For learning audio-video-text representations, conventional single-anchor models struggle when the anchoring modality is absent. For example, text-anchored LanguageBind underperforms in audio-video tasks, while image-anchored ImageBind[33] performs poorly in audio-text tasks (see Tab. 3). These limitations stem from asymmetry due to mismatched cross-modal data scales and the inherent brittleness of binding all modalities to a single hub.

To address this, we develop an audiovisual data engine that *generates missing audio, video, and audio-visual captions* at scale and strengthens alignments between *all* modality pairs. Current visual captioners can accurately describe details and enable efficient data scaling while audio captioners remain weak. Therefore,

we leverage multiple weak audio captions along with video captions, and apply LLM-rewriting to improve coverage and quality of captions.

This richer supervision enables scaling the contrastive objective to cover *more* cross-modal pairs; empirically, increasing the number of pairs consistently improves cross-modal alignment (Tab. 10). Practically, we designed a two-stage data engine described below.

Stage-1: Synthetic Captioning Pipeline. As shown in Fig. 3 stage-1 synthetic captioning pipeline uses Llama 3.1 8B [58] to combine outputs from two weak audio captioning models, EnCLAP [47] and CoNeTTE [49], along with the corresponding confidence scores from Joint-CLAP[91] and video captions. We use the pipeline to generate captions for $O(100M)$ videos chunked at 30-second intervals.

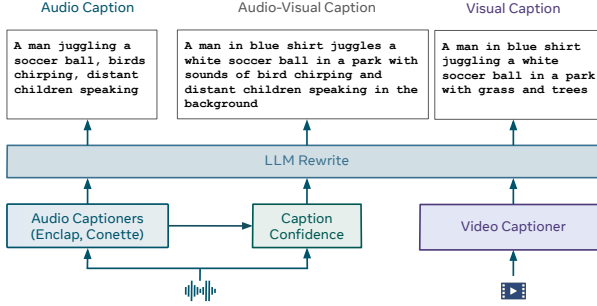
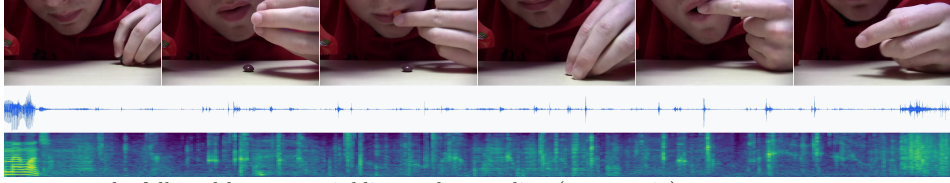


Figure 3 Data Engine: Stage-1 Synthetic Captions: In the first stage we use a synthetic captioning pipeline that uses Llama 3.1 8B to combine information from weak audio captioning models together with confidence using the Joint-CLAP [91] and video captioner to generate audio, visual, and audio-visual captions.

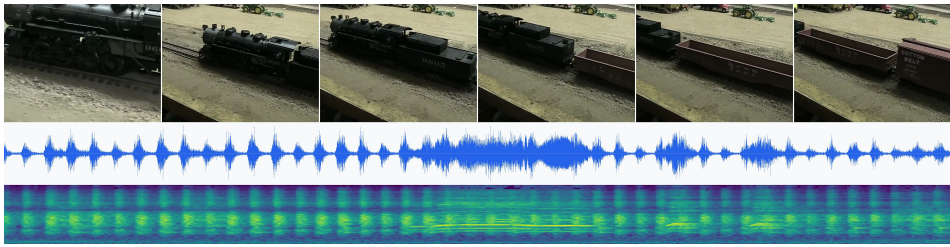
Fig. 4 shows the captions for EnCLAP, CoNeTTE, and our internal video captioning model. We find that (1) EnCLAP and CoNeTTE tend to make different errors, which are reflected in the confidence scores of a CLAP-based model, and (2) video captions can provide useful text context, *e.g.* TV-show, to help disambiguate audio events and improve caption quality. With these observations, we prompt an LLM to combine information from audio and video captions along with discretized confidence scores (low/medium/high) to rewrite audio, visual, and audio-visual caption. Summarizing the visual captions also reduces some LLM decoding errors present in raw video captions. In a small-scale blind subjective evaluation on ~ 50 utterances, LLM audio captions are strictly better than EnCLAP on **65.2%** of utterances, similar on **28.3%**, and worse only on **6.5%**.

Stage-2: Improved Audio and Visual Captions. Fig. 5 shows the second stage pipeline to fuse and improve the audio and visual captions from the first stage. To improve video captions, we utilize the video data engine—a PLM-based model [22] used in PE [8] that focused on fine-grained spatial-temporal visual events. This model processes video metadata along with 32 sampled frames to produce fine-grained video captions. Next, we employ Llama 3.1 (8B) [58] to summarize both the stage-1 output and the fine-grained PLM captions, resulting in the final improved video captions. Similarly, for audio captions, we follow the PLM recipe [22] to train an early version of PLM-AV, a multimodal LLM with a PE_{AV} trained on stage-1 synthetic captions as the audio-visual encoder and Llama [58] as the text decoder. We focus on improving audio understanding with additional visual context.

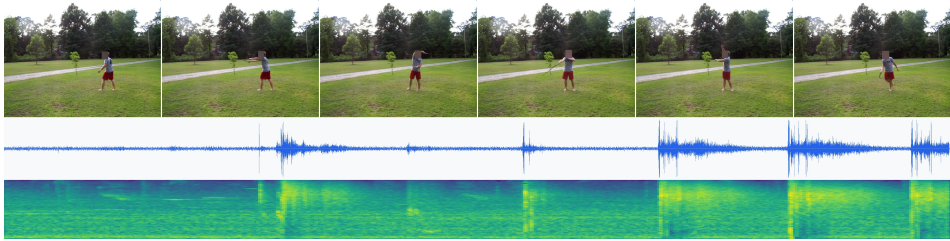
Furthermore, we include speech-related attributes—transcript, language ID (LID), and accent—to enhance PE_{AV}'s capability in speech processing. We use Whisper Large-v3 and Medium ASR models [74] and keep only English transcripts where the two agree (low word error rate). Similarly, we create LID labels with MMS LID models with 126 and 256 languages [72], and keep the labels where the two models share the top-1 prediction. For accent, we train an English accent classifier on Common Voice 13 [2] and apply it to clips with English LID. During training, we randomly inject transcript, LID, and accent into the audio caption, and assign transcripts to a subset of data, always replacing the original caption; this improves transcript retrieval without degrading other tasks. Fig. 6 presents examples of the raw and two-stage processed captions.



EnCLAP: a man speaks followed by some crinkling and crumpling (score: 0.48)
 CoNeTTE: a man is speaking and chewing on something (score: 0.57)
 Video: The video shows a close-up shot of a man eating a small, round candy. In the background, he sits at a white table. The man has fair skin, brown hair and a red shirt. He sits at the table with his hands resting on the edge. He holds an orange candy in his hand to the right. The candy has a blue wrapper with white writing on it. The man puts the candy in his mouth. He chews the candy and swallows it. He then picks up a brown candy from the table. He puts the brown candy in his mouth. He chews the candy and swallows it. He then picks up another orange candy from the table. He puts the orange candy in his mouth. He chews the candy and swallows it. He then picks up another brown candy from the table. He puts the brown candy in his mouth. He chews the candy and swallows it. He then picks up another orange candy from the table. He puts the orange candy in his mouth. He chews the candy and swallows it. The video ends with the man chewing the candy.



EnCLAP: a train is chugging along and a steam whistle goes off (score: 0.50)
 CoNeTTE: a person is using a wrench on a typewriter (score: -0.08)
 Video: The video shows a train traveling on a track. The train has a large, black engine with a black caboose behind it. The caboose has white lettering on the side that reads "COTTON BELT" and "9605." The train is traveling on a track that runs along the bottom of the frame. The background shows a sandy area with several pieces of farm equipment. The video begins with the train traveling toward the left side of the frame. As the video progresses, the train continues to travel along the track. The video ends with the train moving toward the left side of the frame.



EnCLAP: a toy helicopter is flying around and making a lot of noise (score: -0.02)
 CoNeTTE: a whip is being struck in the distance while birds are chirping in the background (score: 0.43)
 Video: The video shows a young man playing with a whip in a grassy field. In the background, there is a gravel path and a line of trees with a house behind them. The man has fair skin and short brown hair. He is wearing a gray t-shirt and red shorts. The whip is long and thin. At the beginning, the man faces the right side of the video while holding the whip in his hand on the left side of the video. He swings the whip over his head and releases it. It whips around the man's body, then moves back toward the camera. The man moves toward the camera as the whip approaches. He catches the whip with his hand on the right side of the video and swings it over his head. The whip whips around the man's body, then moves back toward the camera. The man catches the whip with his hand on the left side of the video. The video is shot by a handheld camera.

Figure 4 EnCLAP and CoNeTTE captions often provide complementary information and the confidence scores reflect the accuracy reasonably, making them favorable to combine with an LLM. Video captions provide strong context. Together this provides strong audio and visual cues for LLM rewriting.

2.2 PE_{AV} Model and Training

Architecture. PE_{AV} builds on pre-trained feature extractors—Perception Encoder [8] for video frames, DAC-VAE [71] for audio, and ModernBERT [95] for text—to obtain video, audio, and text tokens, which are then encoded for contrastive learning. For video encoding, we use PE-L as the frame encoder to extract embeddings

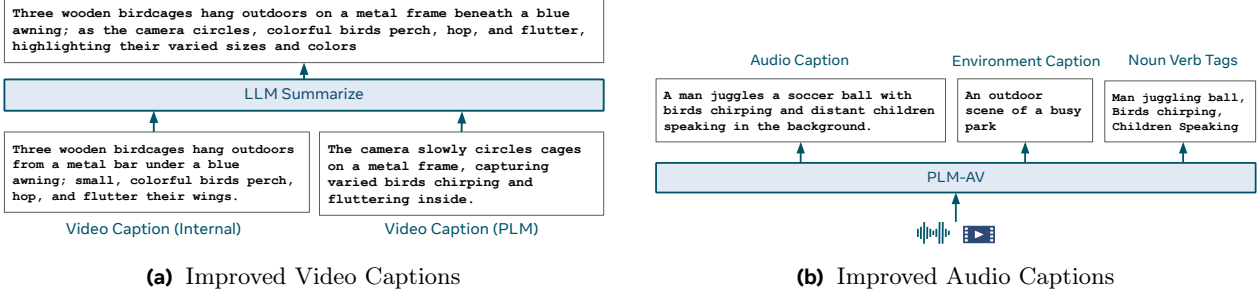


Figure 5 Data Engine: Stage-2 Improved Captions: We improve both the audio and visual captions in the second stage. For the visual captions, we use PLM [22] to generate the video captions and an LLM to summarize the first stage and PLM captions. For audio captions, we follow the PLM recipe [22] to train a PLM-AV model to generate three different audio caption variants focused on audio events, caption, and acoustic environment.

at 30 frames-per-second (FPS). For audio encoding, we extract audio tokens using DAC-VAE at 25 Hz. For text encoding, we leverage ModernBERT with a context length of 512 and use the 22nd layer, which we found to adapt better to audio and speech tasks than the original PE-L text encoder.

More formally, let x^a , x^v , x^t denote raw audio, video, and text inputs, respectively. We first extract the sequential features as follows:

$$\begin{aligned}\mathbf{x}^a &= \text{DAC-VAE}(x^a) \in \mathbb{R}^{L_a \times C_a} \\ \mathbf{x}^v &= \text{PE-L}(x^v) \in \mathbb{R}^{L_v \times C_v} \\ \mathbf{x}^t &= \text{ModernBERT}(x^t) \in \mathbb{R}^{L_t \times C_t}\end{aligned}$$

where $C_a = 128$, $C_v = 1024$, and $C_t = 1024$ are the feature dimensions of DAC-VAE, PE-L, and ModernBERT, respectively, and L_a , L_v , and L_t are the corresponding sequence lengths. For a 30-second clip with 25 Hz audio features and 30 FPS video frames, we have $L_a = 750$ and $L_v = 900$.

For text, we use the [CLS] token from ModernBERT. For audio encoding, we first concatenate a learnable [CLS] token to the projected DAC-VAE tokens. We input this sequence into a N -layer audio Transformer $T_a(\cdot)$ with rotary positional embeddings (RoPE) [83]. The hidden dimension of the audio Transformer is set to $64N$. To further capture temporal context in videos, we concatenate a [CLS] token to the projected frame embeddings, and use a shallow Transformer $T_v(\cdot)$ as the video encoder. The video Transformer shares the same configurations as the audio Transformer except for depth. For brevity, we do not formalize the increasing sequence length of one by the [CLS] tokens. The encoded audio and video are denoted as:

$$\begin{aligned}\mathbf{e}^a &= T_a(\text{Proj}(\mathbf{x}^a)) \in \mathbb{R}^{L_a \times C_e} \\ \mathbf{e}^v &= T_v(\text{Proj}(\mathbf{x}^v)) \in \mathbb{R}^{L_v \times C_e}\end{aligned}$$

where C_e is the dimension of the transformer outputs.

Subsequently, we temporally align the video to the audio tokens using nearest-neighbor interpolation:

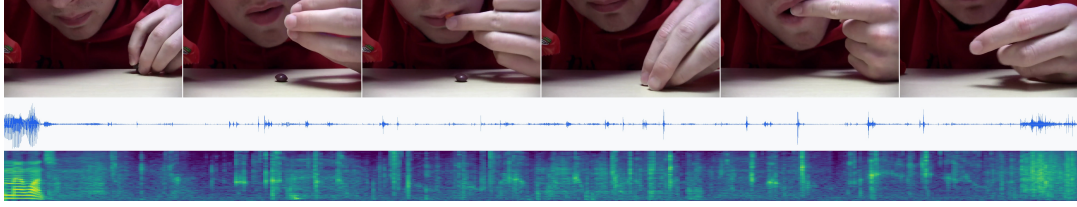
$$\begin{aligned}\tilde{\mathbf{e}}^v &= \text{NearestNeighbor}(\mathbf{e}^a, \mathbf{e}^v) \in \mathbb{R}^{L_a \times C_e} \\ \tilde{\mathbf{e}}^{av} &= \text{Proj}(\text{ChannelConcat}(\mathbf{e}^a, \tilde{\mathbf{e}}^v)) \in \mathbb{R}^{L_a \times C_e}\end{aligned}$$

where $\text{ChannelConcat}(\cdot, \cdot)$ concatenates along the channel dimension, and $\text{Proj}(\cdot)$ produces a audiovisual representation.

We then prepend a learnable [CLS] token and process the sequence with a shallow Transformer $T_{av}(\cdot)$ that models joint audiovisual context and produces the fused audiovisual feature for contrastive learning:

$$\mathbf{e}^{av} = T_{av}(\tilde{\mathbf{e}}^{av}) \in \mathbb{R}^{L_a \times C_e}$$

To compute the contrastive loss, we extract the [CLS] outputs from each encoder—text, audio, video, and audio-video. For captions, we use three separate text projection heads for audio, video, and audio-video



Type	Caption
Audio	A man is speaking and eating candies, accompanied by the sounds of crinkling and crumpling wrappers.
Video	A man with fair skin, brown hair, and a red shirt eats various candies at a white table, alternating between orange and brown candies with blue and white wrappers.
Audio-Visual	The video shows a man eating various candies at a table, with sounds of him speaking and chewing. He picks up and consumes multiple orange and brown candies with blue and white wrappers, accompanied by some sounds of crinkling and crumpling.



Type	Caption
Audio	A police vehicle is moving, triggering a siren, as cars drive by on the city streets.
Video	A purple car with blue and black design drives through the city, passing a black and white police car with flashing red and blue lights, a black and red car, and a white and black car, with the city's buildings, road, and pedestrians in the background.
Audio-Visual	The video shows a purple car racing through the streets of a city, passing by various other cars, including a police car with flashing red and blue lights. The audio captures the sound of a police siren being triggered and a vehicle moving.

Figure 6 Examples of Audio, Video, and Audio-Visual captions generated using the data engine.

captions, yielding $\mathbf{h}^{t_a}, \mathbf{h}^{t_v}, \mathbf{h}^{t_{av}}$, while the audio, video, and audio-video encoders are projected to $\mathbf{h}^a, \mathbf{h}^v, \mathbf{h}^{av}$ in the same shared embedding space. Here, all \mathbf{h} vectors are in \mathbb{R}^{C_h} where C_h is the dimension of the shared embedding space set to 1024 for all model variants.

In addition, to enable text-conditioned cross-modal retrieval (V+T→A, A+T→V)—where the text supplies cues or intent that may be missing in the raw query—we compose the query modality with text to form jointly encoded features. Specifically, given class embeddings $\mathbf{c}^a, \mathbf{c}^v$, and \mathbf{c}^t for audio, video, and text, we perform channel concatenation with text and project to the shared space to obtain

$$\begin{aligned}\mathbf{h}^{vt} &= \text{Proj}(\text{ChannelConcat}(\mathbf{c}^v, \mathbf{c}^t)) \in \mathbb{R}^{C_h}, \\ \mathbf{h}^{at} &= \text{Proj}(\text{ChannelConcat}(\mathbf{c}^a, \mathbf{c}^t)) \in \mathbb{R}^{C_h}.\end{aligned}$$

We include these joint features in stage-2 fine-tuning (Tab. 1) and contrast them with \mathbf{h}^a and \mathbf{h}^v . This enables text-conditioned retrieval such as V+T→A (e.g., retrieving the correct music for a video using text describing the mood) and A+T→V.

Training Objectives. For any modality pair, we pre-train using a sigmoid contrastive objective, similar to [108], to align the corresponding embeddings. Formally, let \mathbf{h}_b^a and \mathbf{h}_b^v denote the embeddings for the b -th sample for the modalities a and v , respectively, and let B denote the batch size. We then calculate the following sigmoid contrastive loss for the alignment of the modalities:

$$\mathcal{L}(\mathbf{h}^a, \mathbf{h}^v) = -\frac{1}{B} \sum_{b=1}^B \sum_{b'=1}^B \log \sigma \left(z_{bb'} \left(-\alpha_{av} \mathbf{h}_b^a \cdot \mathbf{h}_{b'}^v + \beta_{av} \right) \right), \quad (1)$$

where α_{av} and β_{av} denote the temperature and the bias for the pair of modalities a and v . $z_{bb'}$ is the indicator function; $z_{bb'} = 1$ when $b = b'$ and $z_{bb'} = -1$ elsewhere.

We compute the contrastive loss across the following pairs: (1) Audio to audio caption; (2) Audio to video; (3) Audio to audio-video caption; (4) Audio-video to audio caption; (5) Audio-video to audio-video caption; (6) Video to audio caption; (7) Video to video caption; (8) Video to audio-video caption. As to be shown in Tab. 10, we observe that maximum performance is achieved when considering all the pairs of modality and caption types.

In the fine-tuning stage, we additionally include two joint embeddings: (9) Audio with video-caption to video; and (10) Video with audio-caption to audio, leading to ten pairs in total. These additional pairs provide finer control over using only text, video, or audio for retrieval and enable applications such as retrieving the correct music for a video using text describing the mood.

Training Data. We employ a 2-stage training recipe. In the stage-1 pre-training, we focus on scaling the training data with a diverse collection of audio and video samples at scale. We exploit an audiovisual data engine developed in §2.1 to generate different types of refined synthetic captions (audio, video, and audiovisual) for audio and video data without annotations. In addition, we incorporate real captions from public datasets for training. In total, we use 92M unique audio and video samples for stage-1.

In the stage-2 fine-tuning, we utilize a smaller training set well-balanced across domains and modalities. We adjust the data distribution with an emphasis on 1) speech data and the corresponding transcripts, and 2) video data. For the speech data, we include annotated English speech corpora to improve PE_{AV}'s capability in speech transcript retrieval. We observe that a short fine-tuning schedule is sufficient to achieve effective speech-to-transcript association. For the video data, inspired by [8, 68, 73, 100], we include a subset of video-text data by curating videos that contain important visual concepts from the stage-1 videos as well as from [8, 22]. We up-sample these videos for fine-tuning. Overall, we use 32M unique audio/video samples for fine-tuning. Tab. 1 summarizes the composition of the training data. In addition, we fine-tune PE_{AV} with contrastive objective at audio-frame-level to enable fine-grained sound-to-text alignment, dubbed as PE_{A-Frame}, for speech event detection (SED) described next.

3 PE_{A-Frame}: Audio-Frame Level Language Alignment

Typical language–audio models produce a single utterance-level embedding (a global token) for each modality. Then, they apply a contrastive loss to the global class tokens, which achieves coarse-grained cross-modal alignment but overlooks fine-grained interactions. As a result, the correspondence between audio at the frame-level and language remains underexplored, leading to low performance on tasks requiring detailed temporal alignment. To address this limitation, we propose *Perception Encoder Audio-Frame* (PE_{A-Frame}), a model fine-tuned from PE_{AV} with a frame-level audio to language contrastive loss.

Training. We train PE_{A-Frame} to predict the specific frames within an audio signal x^a that contain the sound described by the free-form text description x^t . Building on the pre-trained PE_{AV} model, we fine-tune frame-level audio and instance-level text encoders by adopting a frame-level variant of the sigmoid contrastive loss [108]. For each frame l , we compute the logit between the frame-level audio embedding \mathbf{e}_l^a and the global text embedding \mathbf{h}^{t_a} as $\tilde{h}_l = \mathbf{e}_l^a \cdot \mathbf{h}^{t_a}$.

Input Data and Ground-Truth Label. Each element in a batch of size B consists of an audio sample x_b^a and a single sound event described by its associated text description x_b^t . Although an audio clip may contain multiple sound events, we sample only one text description per element in each batch to simplify implementation. Nevertheless, we provide all annotated sound events and their corresponding frame-level activity masks for every audio sample. Accordingly, each batch element contains

- an audio clip x_b^a ,
- a sampled text query x_b^t describing one sound event in x_b^a , and
- an event-activity mask m_b encoding all annotated events for x_b^a .

For the b -th audio with K_b annotated events $\{x_{b,1}^t, \dots, x_{b,K_b}^t\}$, we define $m_b \in \{0, 1\}^{L_a \times K_b}$, where $m_{b,l,k} = 1$ indicates that event $x_{b,k}^t$ is active at frame l . Even though only one text query per audio is used for contrastive learning, we leverage all annotated events and their *ontology-aware*¹ semantic expansions to construct frame-level supervision.

Let $\text{Ont}(x^t)$ be the set of ontology-linked variants of event x^t (e.g., “speech” includes “female speech”, and “dog” includes “barking”). Then, for each audio frame l in x_b^a and each text query $x_{b'}^t$ in the batch, we assign:

$$z_{b,l,b'} = \begin{cases} +1, & \exists k \in \{1, \dots, K_b\} : x_{b,k}^t \in \text{Ont}(x_{b'}^t) \text{ and } m_{b,l,k} = 1, \\ -1, & \text{otherwise.} \end{cases} \quad (2)$$

Thus, semantically equivalent sound expressions activate the same frames in supervision, improving robustness to linguistic variation and reinforcing hierarchical concept generalization.

Frame-Level Objective. For this task, the model must learn not only *which* sound events are present in an audio clip but also *when* they occur over time. To capture both aspects, we employ two complementary objectives: a *local-activity loss* (computed per batch item) that emphasizes fine-grained temporal localization, identifying *when* events occur within each audio sample, and a *global-activity loss* (computed across the batch) that introduces contrastive context between samples to determine *which* events are active. The local-activity loss helps the model detect event boundaries, while the global-activity loss promotes global event understanding and cross-sample alignment.

The resulting local-activity loss (per-batch-item) yields logits of shape (B, L) , while the global-activity loss (across-batch) yields (B, L, B) :

$$\tilde{h}_{b,l(b')} = \begin{cases} \mathbf{e}_l^a(x_b) \cdot \mathbf{h}^{t_a}(x_b^t) & \text{(local-activity)} \\ \mathbf{e}_l^a(x_b) \cdot \mathbf{h}^{t_a}(x_{b'}^t) \forall, b' \in 1, \dots, B & \text{(global-activity),} \end{cases} \quad (3)$$

A learnable logit scale α and bias β are applied to obtain the final scaled logits $h = \alpha \tilde{h} + \beta$. The frame-level SigLIP loss is computed over these logits. For the local-activity case, the loss is defined as

$$\mathcal{L} = -\frac{1}{BL} \sum_{b,l} \log \sigma(z_{b,l}(\alpha \tilde{h}_{b,l} + \beta)), \quad (4)$$

where $z_{b,l} \in \pm 1$ is the binary label indicating whether frame l of audio x_b^a corresponds to the paired text x_b^t . This formulation naturally generalizes to the global-activity case by computing the loss over $\tilde{h}_{b,l,b'}$ and averaging across all text queries $x_{b'}^t$ in the batch. During training, we probabilistically sample between the two objectives at each iteration, with the probability p_{local} for the local-activity loss. This stochastic choice allows the model to balance precise event-boundary detection and global event activity modeling.

Training Data. For training PE_A-Frame, we use a combination of real-world audio mixtures annotated by humans and synthetic mixtures automatically generated from diverse isolated audio sources. To enhance robustness to reverberation and spatial variability, the audio mixtures are convolved with room impulse responses collected from a variety of acoustic environments. This process allows the model to better generalize across different recording conditions and scene types.

Type	Duration [hours]		Sound Events	
	Real	Synthetic	Real	Synthetic
Speech	0.4 k	0.3 k	70.3 k	108.7 k
Music	0.2 k	0.2 k	0.4 M	0.4 M
General	0.6 k	12.3 k	0.8 M	4.1 M
Total	1.2 k	12.8 k	1.3 M	4.6 M

Table 2 PE_A-Frame Training Data. Durations and sound event counts for real and synthetic recordings across three sound-type categories.

¹By “ontology” we mean a hierarchical taxonomy of sound event labels, such as the AudioSet ontology.

Table 2 provides a summary of the training data, reporting the total durations and number of sound events for both real and synthetic recordings. The *Speech* and *Music* subsets correspond to data explicitly annotated with these categories, whereas the *General* subset comprises a broader range of sounds, which may also include speech or music instances not specifically labeled as such. We use dataset-specific sampling ratios to ensure a balanced mixture of sound events, avoid over-representation, and maintain comprehensive coverage.

4 PE_{AV} Experiments

4.1 Experimental Setups

Datasets. We evaluate PE_{AV} under the zero-shot setting across sound, music, speech, and video benchmarks. For sound and music, we use VGGSound [14], GTzan [90], US8K [75], NSynth [28], ESC50 [70] and CREMA-D [10] classification. AudioCaps [46], Clotho-V2 [25], and VALOR [17] are used for sound-text retrieval. Additionally, we use an internal video dataset for video-to-music retrieval. Unlike public datasets such as VGG-Sound and AudioCaps, where video durations are around 10 seconds, the internal dataset exhibits durations ranging from 5 to 30 seconds. We observe that models trained with a fixed number of frames tend to underperform on audio-to-video retrieval when input durations vary widely. For speech tasks, we use Dynamic-SUPERB [107] to evaluate speech classification on accent, language identification (LID), speech emotion (EMO), and vocal sound detection. VCTK [103] is used for speech-to-transcript retrieval. For video tasks, we have Kinetics-400 [45], Kinetics-700 [11], and HMDB [48] for classification, and MSR-VTT [101], MSVD [13], ActivityNet [9] and DiDemo [1] for video-text retrieval.

Evaluation Protocols. We integrate public baselines and evaluate them using the same evaluation pipeline for a fair comparison,. Following [8, 20], we apply Dual Softmax Loss [21] to re-weight retrieval results. For pre-training, we employ the zero-shot protocol to deduplicate and exclude samples from downstream datasets. For fine-tuning, we consider two protocols: one using only out-of-domain (OOD) data, and another that additionally includes training splits from downstream datasets to match prior setups (*e.g.*, CLAP [96]) for fair comparison on audio benchmarks.

4.2 Main Results

Zero-Shot Sound, Music, and Speech Results. Tab. 3 reports zero-shot classification and retrieval results on sound, music, and speech benchmarks. We compare PE_{AV} with recent audio encoders including CLAP [96], CLAP-Fusion [47], MS-CLAP [27], M2D-CLAP [67], and AudioFlamingo2 [32], and audio-visual encoders including ImageBind [33] and LanguageBind[111]. As illustrated in the last two rows, the proposed two-stage training improves PE_{AV}’s performance, yielding substantial gains in stage-2 fine-tuning when additional speech and video data are incorporated—especially for speech-to-transcript retrieval in VCTK (16.7→85.6 R@1). Notably, the small, base, and large versions of PE_{AV} consistently and significantly outperform all baselines across all zero-shot sound, music, and speech benchmarks. Even under the out-of-domain (OOD) setup, PE_{AV} outperforms other baselines (*e.g.* CLAP and AudioFlamingo2) trained with in-domain data. This represents a notable achievement: to the best of our knowledge, PE_{AV} is the first audio-video-text encoder to achieve state-of-the-art results on *all* types of sound tasks, surpassing both audio-focused (*e.g.* CLAP [27, 67, 96, 104]) and audio-visual models [33, 111].

PE_{AV} demonstrates strong zero-shot performance in both retrieval and classification tasks for sound. For instance, PE_{AV} achieves a state-of-the-art text-to-audio retrieval score of 45.8 R@1 on AudioCaps and 35.1 R@1 on VALOR. Notably, in the zero-shot setup, where PE_{AV} is trained using only out-of-domain (OOD) data, it still significantly outperforms baseline models such as CLAP—even those trained directly on in-domain downstream data like AudioCaps for downstream tasks. PE_{AV} also demonstrates superior performance across different audio types: it achieves strong performance in video-to-music retrieval (our internal benchmarks) and speech-to-transcript retrieval in VCTK. For sound classification on NSynth, GTzan, and ESC50, PE_{AV} also establishes new state-of-the-art performance. Furthermore, PE_{AV} significantly outperforms existing audio-visual baselines in audiovisual retrieval tasks. For example, on AudioCaps video-to-audio retrieval, PE_{AV} achieves 88.3 R@1 compared to 9.1 R@1 for LanguageBind [111] and 51.3 R@1 for ImageBind [33]. The similar trend is observed in VGGSound and our internal music benchmark.

Table 3 Zero-Shot Audio Results. A: Audio, V: Video, T: Audio/Video Caption, PT: pre-training only. OOD: fine-tuning with out-of-domain data only (clearn zero-shot setup). We report recall@1 for retrieval tasks and top1 accuracy for classification tasks. Note that for fair comparison, we integrate baselines into our evaluation pipeline and update their improved results under the same evaluation protocol.

These results highlight the limitations of single-anchor training when binding multiple modalities. For example in AudioCaps, text-anchored LanguageBind performs poorly on VGGSound V→A retrieval (1.6 vs 48.3 R@1 by PE_{AV}) when text input is absent. Also, image-anchored ImageBind underperforms on AudioCaps T→A retrieval (6.6 vs 45.8 R@1 by PE_{AV}) when video input is missing. By scaling the coverage of cross-modal pairs and caption types with an audiovisual data engine, PE_{AV} closes the modality gap and generalizes better.

Another new capability PE_{AV} offers is transcript retrieval. As shown in column VCTK, all the baselines fail to perform this task, leading to a zero recall rate. With transcripts included in the pre-training stage, PE_{AV} shows some capability in transcript retrieval. After fine-tuning, PE_{AV} delivers significant gains (from 16.7 to 85.6 R@1), demonstrating the importance of including speech data in the fine-tuning stage. Furthermore, PE_{AV} outperforms baseline models in most speech-related classification tasks. With pseudo-labeled LID and accent in the pre-training dataset, PE_{AV} offers superior accuracy in language identification and accent classification even without fine-tuning.

Zero-Shot Video Results. We evaluate PE_{AV} on zero-shot video classification and retrieval benchmarks by employing its video-level embedding \mathbf{h}^v of the video encoder as well as the text embedding h^{tv} of the text encoder. By default PE_{AVL} is trained and evaluated under 30 fps. We also report performance of PE_{AVL} trained and evaluated with a fixed number of 16 frames with improved computational efficiency. PE_{AV} at 30 fps achieved better performance. Note that all video results adhere to the clean zero-shot (OOD) setup, with no samples from downstream datasets used.

As shown in Tab. 4, PE_{AV}L achieves an overall +10.8 R@1 improvement in retrieval and a +5.0 accuracy gain in classification over PE-L. PE_{AV}L even surpasses PE-G—a model with 4× more parameters—by +6.5 R@1 in retrieval and +1.6 accuracy in classification. This trend also holds consistently under the 16-frame sampling setting with a lower computation cost. We attribute PE_{AV}’s superior performance to its lightweight temporal Transformers which effectively capture temporal context across longer video frames, and its broader coverage of audio-video data, particularly the inclusion of longer and semantically rich videos. These improvements significantly boost text-video retrieval in ActivityNet (+20.1 T→V, +25.6 V→T R@1) over PE-L.

Compared to other baselines, PE_{AV}L also yields a notable +5.7 accuracy improvement in zero-shot classification compared to prior SOTA model (InternVideo2 [94]) and recent vision encoders such as SigLIP2 [87]. Notably, PE_{AV} achieve these with significantly much fewer parameters compared to baselines such as InternVideo2 [94], VideoPrism [110] and PE-G [8]. PE_{AV} successfully set new state-of-the-art performance in zero-shot classification and retrieval for video, sound, music and speech benchmarks.

Model	V-Enc Params.	Video Data	Resolution	Frame/fps [*]	Zero-Shot Retrieval										Zero-Shot Classification							
					Avg Retrieval		VTT $T \rightarrow V$ [101]	VTT $V \rightarrow T$ [101]	MSVD $T \rightarrow V$ [13]	MSVD $V \rightarrow T$ [13]	ActivityNet $T \rightarrow V$ [9]	ActivityNet $V \rightarrow T$ [9]	DiDeMo $T \rightarrow V$ [1]	DiDeMo $V \rightarrow T$ [1]	VATEX $T \rightarrow V$ [93]	VATEX $V \rightarrow T$ [93]	Avg Class.		Kinetics 400 [45]	Kinetics 600 [45]	Kinetics 700 [45]	Kinetics UCF 101 [82]
<i>Baselines</i>																						
UMT-L [51]	0.3B	25M	224	8	-	40.7	37.1	49.0	74.5	41.9	39.4	48.6	49.9	-	-	-	-	-	-	-	-	
ImageBind [33]	0.6B	3M	224	16	48.7	40.6	42.9	47.9	70.9	36.6	34.1	36.0	38.2	69.8	69.8	54.4	55.0	53.5	42.7	77.1	43.8	
LanguageBind [111]	0.3B	10M	224	16	58.3	48.6	48.7	55.6	78.8	48.0	48.8	43.5	44.7	82.9	83.1	63.5	64.3	63.4	55.4	81.3	53.0	
SigLIP2-L/16 [87]	0.3B	n/a	384	8	47.1	41.5	31.4	53.7	74.2	35.9	31.5	36.6	37.8	64.1	64.3	64.1	65.3	62.5	56.8	86.7	49.3	
InternVL [20]	5.5B	n/a	224	8	-	44.7	40.2	-	-	-	-	-	-	-	-	-	69.1	68.9	60.6	-	-	
InternVideo2 [94]	1.0B	102M	224	8	62.7	51.9	50.9	58.1	83.3	60.4	54.8	57.0	54.3	70.4	85.4	70.7	73.1	72.8	64.9	88.8	53.9	
SigLIP2-g-opt [87]	1.1B	n/a	384	8	49.4	43.1	34.2	55.8	74.6	38.3	33.4	39.2	40.1	67.5	68.2	68.2	69.8	67.0	61.8	90.7	51.8	
PE-G [8]	1.9B	22M	448	8	61.4	51.2	49.9	59.7	85.4	54.7	51.2	45.8	46.5	83.6	85.5	74.8	76.9	76.1	69.1	90.7	61.1	
PE-L [8]	0.3B	22M	336	8	57.1	50.3	50.1	57.2	82.4	46.4	42.1	42.4	41.0	79.0	80.5	71.4	73.4	72.7	65.3	87.1	58.5	
<i>16 Frames</i>																						
PE _{AV} S	0.3B	124M	336	16	65.7	46.7	49.6	60.1	86.4	63.4	64.8	48.7	49.0	94.2	93.7	74.9	77.4	77.0	67.9	87.8	64.6	
PE _{AV} B	0.4B	124M	336	16	65.8	48.6	50.3	60.8	87.6	64.0	64.9	46.2	47.8	94.3	93.8	75.9	77.9	77.8	68.3	89.7	65.9	
PE _{AV} L	0.5B	124M	336	16	66.9	49.0	50.5	60.5	88.4	65.4	66.5	48.9	50.1	94.9	94.4	75.9	78.4	77.9	68.2	89.2	66.0	
<i>30 fps</i>																						
PE _{AV} S	0.3B	124M	336	30 [*]	66.4	49.3	49.4	59.8	87.5	64.8	65.5	50.0	49.0	94.5	94.5	76.3	78.7	78.2	69.1	89.2	66.1	
PE _{AV} B	0.4B	124M	336	30 [*]	66.5	47.7	48.4	60.7	87.6	65.7	65.9	49.3	50.1	94.9	94.4	76.1	78.5	78.2	68.9	89.5	65.7	
PE _{AV} L	0.5B	124M	336	30 [*]	67.9	51.9	51.2	60.8	87.6	66.5	67.7	51.6	51.7	95.1	94.8	76.4	78.9	78.3	69.0	90.4	65.1	

Table 4 Zero-Shot Video Results. Comparison of PE_{AV} with recent video–language encoders. We report recall@1 for retrieval tasks and top1 accuracy for classification tasks. PE_{AV} achieves state-of-the-art results on most classification and retrieval tasks with only 0.3–0.5B parameters.

Joint Modal Analysis. Beyond audio-only and video-only benchmarks, PE_{AV} demonstrates strong potential as a step change towards an omni-modal encoder. In Tab. 5, PE_{AV} jointly incorporates information from multiple modalities and improves upon the best result achieved with a single modality (results marked with \dagger). In all the benchmarks, PE_{AV} significantly outperforms other multimodal baselines, surpassing ImageBind [33] by 42.2% and LanguageBind [111] by 43%, establishing a new state-of-the-art for audio, video, and text encoders.

We observe that joint embeddings are helpful when the input modalities offer complementary information. For audio tasks such as AudioCaps, combining video and text signals ($V+T \rightarrow A$) clearly outperforms either $V \rightarrow A$ or $T \rightarrow A$, yielding a +6.9 R@1 improvement. Similarly, for visual tasks like DiDeMo and VTT, audio-augmented text queries ($A+T \rightarrow V$) outperform $A \rightarrow V$ and $T \rightarrow V$, increasing R@1 by 21.7 and 11.5, respectively. Notably, when audiovisual captions are available (*e.g.* captions in VALOR), PE_{AV} also achieves stronger performance for joint audio-video retrieval compared to single-modal retrieval: 76.8 T→A+V R@1 v.s. 70.9 T→V and 35.1 T→A R@1.

4.3 Ablation Studies

In Tab. 6–10, we ablate PE_{AV}B (16-layer audio Transformer) trained for 100K steps with 800 batch size on pre-training data. ACaps, GTZ, and DSUP denote AudioCaps, GTzan, and Dynamic-SUPERB, respectively.

Model	Avg	Zero-Shot Retrieval						Zero-Shot Classifi.			
		AudioCaps $T, V \rightarrow A$ [46]	VALOR $T \rightarrow A+V$ [17]	VALOR $T+A \rightarrow V$ [17]	VTT $T+A \rightarrow A$ [17]	DiDeMo $T, A \rightarrow V$ [1]	VGGSound $A \rightarrow T$ [14]	VGGSound $V \rightarrow T$ [14]	VGGSound $A+V \rightarrow T$ [14]		
ImageBind [33]	38.0	51.3	36.1	36.1	24.2	41.9	36.1	28.2	40.4	40.4	
LanguageBind [111]	37.2	19.7	46.8	46.8	6.5	50.9	44.2	26.0	45.4	45.4	
<i>16 Frames</i>											
PE _{AV} L \dagger	65.5	86.1	70.9	71.6	71.1	50.7	61.1	-	-	-	47.3
PE _{AV} L	77.5	94.6	76.8	91.6	76.8	73.2	78.3	46.7	47.3	51.0	
<i>30 FPS</i>											
PE _{AV} L \dagger	69.8	88.3	70.9	73.8	74.5	63.6	69.3	-	-	-	48.0
PE _{AV} L	80.2	95.2	76.8	93.0	78.8	85.3	80.8	47.1	48.0	51.8	

Table 5 Zero-shot Joint-Modal Results. For the baselines and PE_{AV} marked with \dagger , joint queries are approximated via maximum over uni-modal results, i.e., $T+V \rightarrow A = \max(T \rightarrow A, V \rightarrow A)$, $T \rightarrow A+V = \max(T \rightarrow A, T \rightarrow V)$, and $T+A \rightarrow V = \max(T \rightarrow V, A \rightarrow V)$. PE_{AV} enables using native joint embeddings $T+V$, $A+V$, and $T+A$ for retrieval and classification. Using joint embeddings is beneficial when content in different modalities complement each other.

Data Engine. Tab. 6 compares captions generated by weak captioner (EnCLAP [47] and CoNeTTE [49]) to the improved captions by Stage-1 and Stage-2 data engine in §2.1. The proposed data engine jointly leverages video captions and confidence scores to improve the quality of audio captions over the raw EnCLAP and CoNeTTE outputs. Moreover, the improved captions from Stage-2 yield further improvements in most sound, speech, and video tasks.

Real vs Synthetic Data. Tab. 7 compares models trained with different real–synthetic caption ratios under a fixed total number of training samples, and shows that using only real captions (row 2) underperforms using only synthetic captions (row 1), indicating that synthetic captions from our audiovisual data engine are high quality and diverse. Rows 2–5 further show that real and synthetic data are complementary: mixed training (row 4) outperforms either alone (rows 1 and 2), with a 1:10 real-to-synthetic ratio yeilding the best results.

Data Scaling. Tab. 8 examines the scaling behavior of the proposed data engine for generating synthetic captions. We fix the data mixing ratio across datasets and data type and scale the data from 2M to 64M. As shown, the model’s performance increases monotonically on average as the data size grows, reaching its peak at 64M samples demonstrating the importance of the diverse audio-visual data.

Model Size Scaling. Tab. 9 scales Transformer layers of the audio encoder from 8 to 28 (0.03–1.11B parameters), while keeping the visual and audio-video encoders fixed. As shown, performance consistently improves with larger and deeper models up to 20 layers under the ablation setup. The scaling trend is important, as it implies strong capacity gains with depth; however, the saturation around 20 layers is likely due to shorter training schedule. The 28 layers model performs the best in the full scale experiment.

Scaling Contrastive Objective. Tab. 10 shows how scaling coverage and types of contrastive loss pairs impact model performance. As can be seen, expanding the contrastive objective to cover a greater number of possible alignments between modalities and caption types leads to improved results. For example, the contrastive objective, when applied to all eight modality-caption pairs, outperforms the audio-text only contrastive training, which is limited to only audio to audio caption pairs. Interestingly, we also find that adding cross-modality pairs for example *video to audio caption* and *audio-visual to video caption* in row 5 leads to improvements in text to video retrieval and zero-shot classification, showcasing the value of richer cross-modal alignment strengthens the shared embedding space. These findings highlight the importance of scaling the coverage of cross-modal alignments

Caption	Sound-Ret.			Sound-Class.			Speech-Class.			Video-Ret.			Video-Class.														
	Acaps			VGG			GTZ			CV-13			DSUP			VTT			ANet			K700			HMDB		
	Avg	T2A	AV2T	Avg	T2A	AV2T	Avg	T2A	AV2T	accent	CV-13	DSUP	lid	T2V	T2V	T2V	T2V	T2V	V2T	V2T	V2T	V2T	V2T	V2T			
EnCLAP	33.1	23.7	19.8	50.5	10.9	24.0	31.3	55.1	38.0	44.7																	
CoNeTTE	35.4	26.8	29.3	55.6	12.2	21.5	31.1	56.8	38.7	46.4																	
Stage-1	38.9	30.3	39.3	57.2	15.1	21.5	36.2	56.8	44.9	49.1																	
Stage-2	41.5	32.2	44.3	59.8	16.8	30.0	36.2	57.7	45.3	51.1																	

Table 6 Data Engine. Compared to off-the-shelf captioners (EnCLAP [47] and CoNeTTE [49]), our data engine significantly improves the data quality by taking into account video context and confidence score.

Real	Syn.	S-Ret.			Sound-Class.			Speech-Class.			Video-Ret.			Video-Class.														
		Acaps			VGG			GTZ			CV-13			DSUP			VTT			ANet			K700			HMDB		
		Avg	T2A	AV2T	Avg	T2A	AV2T	Avg	T2A	AV2T	accent	CV-13	DSUP	lid	T2V	T2V	T2V	T2V	T2V	V2T	V2T	V2T	V2T	V2T	V2T			
0x	1x	43.0	26.1	44.3	60.7	18.1	37.5	32.7	55.4	57.2	55.4																	
1x	0x	14.9	16.4	25.5	58.4	11.3	20.5	0.1	0.0	0.1	0.1																	
1x	1x	40.5	27.1	41.3	65.1	18.5	36.0	29.8	42.3	51.4	52.8																	
1x	10x	45.4	32.5	44.8	62.0	23.5	46.0	32.8	53.8	54.9	58.2																	
1x	20x	43.5	30.6	44.4	63.0	16.8	43.0	33.5	56.1	52.6	51.5																	
1x	30x	44.2	30.8	43.1	58.9	23.1	51.0	33.8	55.1	50.3	51.3																	

Table 7 Data Mixing Ratio. Mixing both types of date performs better than using only real or synthetic data. Higher synthetic ratios (till 1:10) further boost performance by improving diversity.

Data	Data	S-Ret.			Sound-Class.			Speech-Class.			Video-Ret.			Video-Class.														
		Acaps			VGG			GTZ			CV-13			DSUP			VTT			ANet			K700			HMDB		
		Avg	T2A	AV2T	Avg	T2A	AV2T	Avg	T2A	AV2T	accent	CV-13	DSUP	lid	T2V	T2V	T2V	T2V	T2V	V2T	V2T	V2T	V2T	V2T	V2T			
$\mathcal{O}(2M)$	38.4	27.0	40.4	60.2	20.2	36.0	32.8	50.4	36.9	41.6																		
$\mathcal{O}(4M)$	41.8	29.6	43.4	63.9	17.2	41.5	34.9	53.1	40.5	51.7																		
$\mathcal{O}(8M)$	42.0	31.3	44.7	61.8	18.9	39.5	34.5	55.5	42.8	48.8																		
$\mathcal{O}(16M)$	42.9	32.1	45.2	62.1	19.3	41.0	36.2	56.5	43.0	50.3																		
$\mathcal{O}(32M)$	42.8	32.8	45.4	62.0	18.1	39.0	35.6	56.5	43.7	51.9																		
$\mathcal{O}(64M)$	43.4	33.6	46.2	63.8	16.0	43.0	35.6	57.7	43.9	50.7																		

Table 8 Data Scaling. Performance increases and peaks at 64M, underscoring the value of diverse audio-visual data.

A-layers	A-params	V-params	S-Ret.			Sound-Class.			Speech-Class.			Video-Ret.			Video-Class.			Acap			VGG			GTZ					
			Acaps			VGG			GTZ			CV-13			DSUP			VTT			ANet			K700			HMDB		
			Avg	T2A	AV2T	Avg	T2A	AV2T	Avg	T2A	AV2T	accent	CV-13	DSUP	lid	T2V	T2V	T2V	T2V	T2V	V2T	V2T	V2T	V2T	V2T	V2T			
8	0.03B	0.34B	41.1	29.5	45.0	58.0	19.3	32.0	35.8	54.9	44.1	51.2																	
12	0.09B	0.35B	43.3	32.0	45.4	63.1	21.9	38.0	36.6	56.3	44.5	51.6																	
16	0.21B	0.38B	42.9	32.1	33.2	45.4	61.8	19.3	41.0	36.6	56.3	43.6	48.9																
20	0.41B	0.42B	44.5	34.4	46.2	62.8	21.9	44.0	37.3	56.7	44.6	52.4																	
24	0.70B	0.45B	43.1	34.4	45.7	62.6	22.7	38.0	35.2	55.7	43.7	50.1																	
28	1.11B	0.50B	42.0	34.3	44.9	65.0	16.0	34.0	35.5	56.7	43.0	49.0																	

Table 9 Scaling Audio Encoder. Scaling audio encoder improves performance, with saturation beyond ~20 layers likely due to limited data and training steps.

A-V	A-AT	A-VAT	V-VT	S-Ret.			Sound-Class.			Speech-Class.			Video-Ret.			Video-Class.								
				Acaps			VGG			GTZ			CV-13			DSUP			VTT			ANet		
				Avg	T2A	AV2T	Avg	T2A	AV2T	Avg	T2A	AV2T	accent	CV-13	DSUP	lid	T2							

for learning aligned audio, visual, and text representations. PE_{AV} achieves its peak performance when the contrastive objective considers eight possible cross-modal pairings.

4.4 Qualitative Results

Fig. 7 and 8 demonstrate qualitative video→text and text→video retrieval results by PE_{AV}. In Fig. 7, the ground truth video is successfully retrieved, while the top 2 and 3 retrieved videos show similar scenarios as well (water sports). Fig. 8 shows a similar phenomenon, but retrieved in the opposite direction. These examples showcase PE_{AV}’s natural capabilities for capturing information from unimodal data and aligning content across modalities.

Query: in the ocean a man on a surfboard rides a wave

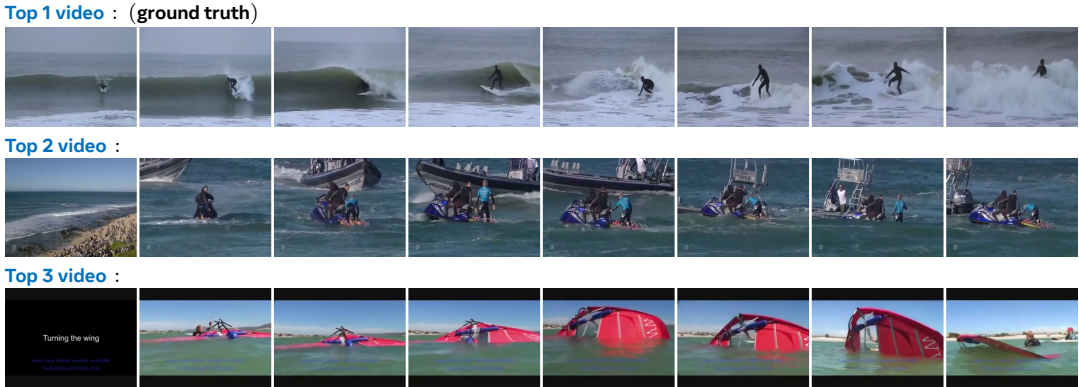


Figure 7 Video-caption → Video retrieval results from PE_{AV}. Ground truth (if present) is bolded.



Top 1: a helicopter moving in air and red and yellow dress man hand touching speaking in snow land wearing helmet displaying on screen (**ground truth**)

Top 2: a man rides a lift to the top of a mountain

Top 3: flight is shaken and the pilots trying to land the flight while they opened the air

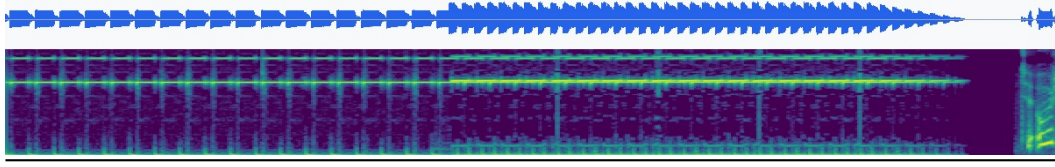
Figure 8 Video → Video-caption retrieval results from PE_{AV}. Ground truth (if present) is bolded.

Next, the following examples demonstrate PE_{AV}’s novel capability to extract and relate multiple modalities. Fig. 9 showcases joint audio+text→video retrieval results. The additional audio context helps break the ties of the video and retrieve the corresponding video correctly compared with using either text or audio as the query. Moreover, in Fig. 10, retrieval based solely on video or audio omits key information. E.g., “audio → text” is unsuccessful because the visual cue of “car” is challenging to extract from the audio. By leveraging joint multimodal retrieval, PE_{AV} incorporates both audio and video context, enabling it to correctly identify the top-1 result.

Furthermore, Fig. 11 demonstrates the speech → audio caption/transcript retrieval capabilities. First, when the audio caption is perturbed (similar and wrong examples), the retrieval score decreases, indicating the success of identifying the correct speaker, speaking style, and recording environment. In the second section, we replace some words in the correct transcript with similar-sounding words and find slightly lower scores. In contrast, rewriting the transcript with different words while preserving meaning significantly decreases scores, implying that PE_{AV} captures pronunciation more than meaning in speech. Moreover, completely irrelevant transcripts lead to even worse scores. The final section shows the case in which both the caption and the transcript are present in the retrieved text. The highest score is achieved when both the caption

Text Query: In the room, a man pressed the alarm with his index finger, and the alarm rang.

Audio Query:



Text → Video



(Caption: A person presses the button of the instrument watch on the wall, and the instrument drips.)

Audio → Video

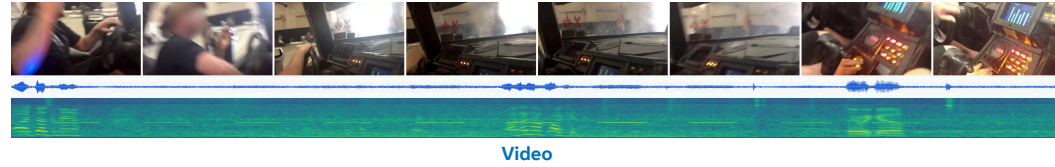


(Caption: In the enclosed space, a mouse whirled in the dripping sound, the picture turned into two rats.)

Text + Audio → Video (ground truth)



Figure 9 $T + A \rightarrow \text{Video}$ retrieval results from PE_{AV}. Ground truth (if present) is bolded.



Video

Audio → Text

Top 1: A man in a life-saving suit stood beside the manhole cover, directing the rumbling engineering vehicle to reverse, and then angling the vehicle's gear to the sewer.

Top 2: In the field, a command officer in a fluorescent green work suit was waving a flag to direct a farm machine vehicle, with the sound and beeping of vehicles and the voice of men.

Top 3: Outside, a man sits in a car talking while driving slowly as the car dribbles. (**ground truth**)

Video → Text

Top 1: A man fiddled with the steering wheel in the driver's seat, making a rustling sound, and the roar of machine operation from time to time in the distance.

Top 2: The man was sitting in the driver's seat talking, the picture shaking, saw the co-pilot and the windows open inside and behind the car.

Top 3: A man is introducing virtual technology to his buddies at the creaking edge of the wheel.

Audio + Video → Text

Top 1: Outside, a man sits in a car talking while driving slowly as the car dribbles. (**ground truth**)

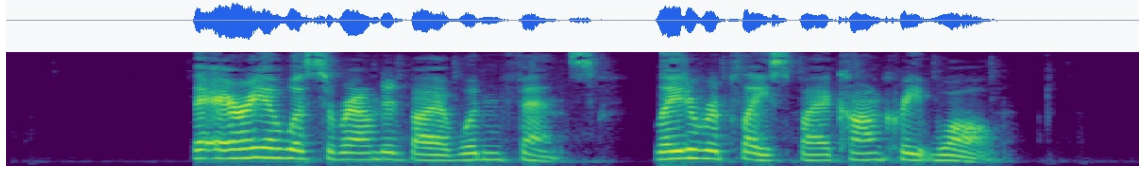
Top 2: A man fiddled with the steering wheel in the driver's seat, making a rustling sound, and the roar of machine operation from time to time in the distance.

Top 3: The man was sitting in the driver's seat talking, the picture shaking, saw the co-pilot and the windows open inside and behind the car.

Figure 10 $A/V/AV \rightarrow \text{AV-caption}$ retrieval results from PE_{AV}. Ground truth (if present) is bolded.

and the transcript are correct, indicating that providing more textual information helps retrieve the desired speech signal. Finally, we replace the captions and transcripts with incorrect ones and find that incorrect transcripts decrease scores the most. The results reveal transcripts have a higher impact on the score than audio descriptions, offering more accurate retrieval between speech and text when the transcript is presented.

Overall, the results strongly suggest the usefulness of PE_{AV} for speech-related tasks.



Caption	Score
Correct: A middle-aged female voice, spoken at a normal pace, with a normal pitch and quality.	0.571
Similar 1: A young female voice, spoken at a normal pace, with a normal pitch and quality.	0.250
Similar 2: A middle-aged male voice, spoken at a normal pace, with a normal pitch and quality.	-0.207
Similar 3: A middle-aged female voice, spoken at a fast pace, with a normal pitch and quality.	0.109
Wrong 1: A young female voice, spoken at a fast pace, with a high pitch and low recording quality.	-0.538
Wrong 2: A middle-aged male voice, spoken at a slow pace, with a low pitch and normal quality.	-0.582
Wrong 3: A young male voice, spoken at a fast pace, with a normal pitch and quality.	-0.739
Transcript	Score
Correct: The person says: "The area was surrounded by a wooden fence, later replaced by a concrete wall."	0.399
Similar Pronunciation 1: The person says: "The era was surrounded by a wooden sense , later replayed by a convict call ."	0.227
Similar Pronunciation 2: The person says: "The aria was confounded by a warden fence, later replaced by a con fleet wall."	0.268
Similar Pronunciation 3: The person says: "The airy was surrendered by a wooden lens , later rephrased by a concrete mall ."	0.172
Similar Meaning 1: The person says: "The yard was enclosed by a timber fence, later swapped for a stone wall."	-0.331
Similar Meaning 2: The person says: "The field was bordered by a wooden fence, which was later rebuilt in concrete."	-0.233
Similar Meaning 3: The person says: "A wooden fence once circled the property, but it was replaced by a solid wall."	-0.478
Wrong 1: The person says: "Man in red tshirt and baseball cap viewed from above he is has a pile of posters."	-0.956
Wrong 2: The person says: "Hash trees allow efficient and secure verification of the contents of large data structures."	-2.469
Wrong 3: The person says: "Armand immigrated to the United States from France and sold hats as an occupation."	-1.981
Caption + Transcript	Score
Correct: A middle-aged female voice, spoken at a normal pace, with a normal pitch and quality. The person says: "The area was surrounded by a wooden fence, later replaced by a concrete wall."	0.984
Wrong Caption + Correct Transcript 1: A young female voice, spoken at a fast pace, with a high pitch and low recording quality. The person says: "The area was surrounded by a wooden fence, later replaced by a concrete wall."	0.170
Wrong Caption + Correct Transcript 2: A middle-aged male voice, spoken at a slow pace, with a low pitch and normal quality. The person says: "The area was surrounded by a wooden fence, later replaced by a concrete wall."	0.205
Wrong Caption + Correct Transcript 3: A young male voice, spoken at a fast pace, with a normal pitch and quality. The person says: "The area was surrounded by a wooden fence, later replaced by a concrete wall."	0.018
Correct Caption + Wrong Transcript 1: A middle-aged female voice, spoken at a normal pace, with a normal pitch and quality. The person says: "Man in red tshirt and baseball cap viewed from above he is has a pile of posters."	-0.536
Correct Caption + Wrong Transcript 2: A middle-aged female voice, spoken at a normal pace, with a normal pitch and quality. The person says: "Hash trees allow efficient and secure verification of the contents of large data structures."	-1.737
Correct Caption + Wrong Transcript 3: A middle-aged female voice, spoken at a normal pace, with a normal pitch and quality. The person says: "Armand immigrated to the United States from France and sold hats as an occupation."	-1.425

Figure 11 Speech → Audio-caption and transcript retrieval results from PE_{AV}. The scores indicate the embedding similarity scores between the [CLS-A] and [CLS-AT].

4.5 Implementation Details

Architecture. Tab. 11 summarize PE_{AV} model configurations. We utilize a pre-trained PE-L [8] as the base frame encoder to capture spatial context and stack 4 lightweight temporal Transformer layers as the video encoder to capture temporal context across frames. For the audio, we encode raw audio using a pre-trained DAC-VAE [71] followed by a Transformer audio encoder, which contains 28 layers and 1.11B parameters in PE_{AVL}. We scale the hidden dimension proportionally to the number of layers with a factor of 64, and adjust the number of heads with a factor of 0.5. The audio-video transformer comprises of 6 layers with the same scaling principle for its hidden size and number of heads. For the text encoder, to support transcript data which requires long context length, we use pre-trained ModernBERT with 28 layers with 512 context length.

Training. We pre-train PE_{AV} for 250K steps using batch size of 3024 and a learning rate of 10^{-4} . We leverage pre-trained PE-L [8] and ModernBERT [95] as the frame and text encoder respectively, and randomly initialize the rest of modules (video encoder, audio encoder, and audio-video fusion encoder). The 92M pre-training data composition is in Tab.1 and the synthetic captions are generated using the audiovisual data engine in §2.1. We pre-train PE_{AVL} on 216 GPUs for around 9 days. For fine-tuning, we train with the same learning rate for 50K steps with 32M data composition described in Tab. 1 under the fine-tuning data. For the out-of-domain setup we exclude 8M data from the public datasets and internal datasets used in the evaluation in Tab. 3-4.

Scale	Tower	Params	Width	Depth	MLP	Heads	Dim
S	Audio	0.09B	768	12	2048	6	1024
	Video (Spatial, PE-L)	0.32B	1024	24	4096	16	1024
	Video (Temporal)	0.03B	768	4	2048	6	1024
	Audio-Video	0.05B	768	6	2048	6	1024
B	Text	0.39B	1024	28	5248	16	1024
	Audio	0.21B	1024	16	2752	8	1024
	Video (Spatial, PE-L)	0.32B	1024	24	4096	16	1024
	Video (Temporal)	0.06B	1024	4	2752	8	1024
L	Audio-Video	0.08B	1024	6	2752	8	1024
	Text	0.39B	1024	28	5248	16	1024
	Audio	1.11B	1792	28	4800	14	1024
	Video (Spatial, PE-L)	0.32B	1024	24	4096	16	1024
	Video (Temporal)	0.18B	1792	4	4800	14	1024
	Audio-Video	0.25B	1792	6	4800	14	1024
	Text	0.39B	1024	28	5248	16	1024

Table 11 Model Configurations. Total Parameters: PE_{AVS}: 0.9B; PE_{AVB}: 1.1B; PE_{AVL}: 2.2B.

5 Downstream Application of PE_{A-Frame}: Sound Event Detection (SED)

We evaluate PE_{A-Frame} on the task of polyphonic sound event detection SED, which is defined as the detection of sound events from multiple classes, where sound events can occur simultaneously [61]. Traditional (closed-vocabulary) SED typically targets a fixed set of classes, predicting a binary label for each class per time frame. In contrast, open-vocabulary SED aims to detect the temporal boundaries of arbitrary sound events conditioned on a free-form textual description [36, 98]. Our model is designed to address both closed- and open-vocabulary SED, supporting free-form textual queries for arbitrary sound events. For closed-vocabulary evaluation, it is prompted with each class from the predefined ontology, and detection proceeds as in the traditional setting. For open-vocabulary evaluation, we assume access to a free-form textual description of the sound events present in the audio, and the model predicts the precise onset and offset boundaries of every instance of the specified events.

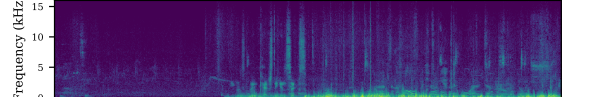
Test sets and metrics. To evaluate performance, we employ both open-vocabulary (Internal Bench, ASFX-SED [97]) and closed-vocabulary test sets (AudioSet-Strong [37], DESED [89]—a.k.a. “Youtube” subset in DCASE19 [88], and UrbanSED [76]), where Internal Bench denotes an internal benchmark. We assess model performance using two threshold-independent metrics: the intersection-based polyphonic sound detection score (PSDS) [7] and the segment-based area under the receiver operating characteristic (AUROC). For open-vocabulary SED datasets, AUROC is computed only over the true positive and false positive rates of events that actually occur in each audio clip. For closed-vocabulary test sets, predictions are generated for all classes included in the respective datasets. We apply a median filter of 9 to the raw predictions and use the `sed_scores_eval` package [26] with parameters $\rho_{DTC} = 0.7$, $\rho_{GTC} = 0.7$, $\alpha_{ST} = 1$, $\alpha_{CT} = 0$, and $e_{max} = 100$, corresponding to the standard PSDS1 configuration [7]. However, consistent with [53, 78], we omit the variance penalty ($\alpha_{ST} = 0$) for AudioSet-Strong, as PSDS was originally designed for datasets with fewer and less imbalanced classes [7]. Following [36], we refer to PSDS1 computed across all classes as PSDS1_A, which emphasizes accurate temporal alignment but still penalizes false positives, and adopt its variant, PSDS1_T, which focuses solely on target sounds.

	Freeform Rate [Hz]	Open-vocabulary SED				Closed-vocabulary SED						UrbanSED (10 classes)		
		Internal Bench		ASFX-SED		AudioSet-Strong (407 classes)			DESED (10 classes)			UrbanSED (10 classes)		
		AUROC	AUROC	PSDS1 _A	PSDS1 _T	AUROC	PSDS1 _A	PSDS1 _T	AUROC	PSDS1 _A	PSDS1 _T	AUROC		
PretrainedSED [78]	X	25	-	-	0.47	0.52	0.98	-	-	-	-	-	-	-
FLAM [98]	✓	3.2	-	0.81	0.35	-	0.95	0.09	-	0.92	0.30	-	-	0.94
FlexSED [36]	✓	25	0.62	0.74	0.45	0.58	0.96	0.16	0.27	0.93	0.05	0.11	0.71	
PE_A-Frame	✓	25	0.91	0.83	0.43	0.61	0.96	0.34	0.58	0.97	0.12	0.22	0.89	

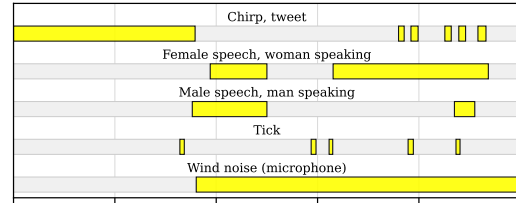
Table 13 Sound Event Detection Results. Performance of PE_A-Frame on open-vocabulary (Internal Bench, ASFX-SED) and closed-vocabulary (AudioSet-Strong, DESED, UrbanSED) SED test sets. PE_A-Frame achieves the best PSDS1_T across all benchmarks, indicating superior temporal localization. PretrainedSED is strong but limited to AudioSet-Strong due to its closed-vocabulary design, while FLAM mainly excels on UrbanSED, likely because it is trained on this synthetic dataset and operates at a coarser 3.2 Hz frame rate.

Baselines. We compare our model with PretrainedSED [78], FLAM [98], and FlexSED [36]. PretrainedSED. We use the best-performing checkpoint based on the BEATs transformer [18] as it includes a final task-specific layer that outputs probabilities for the AudioSet-Strong classes. Its training pipeline employs a balanced sampler, extensive data augmentation, and ensemble knowledge distillation, making it highly optimized for the AudioSet-Strong test set. In contrast, FLAM and FlexSED accept free-form textual descriptions and are therefore also suitable for open-vocabulary SED.

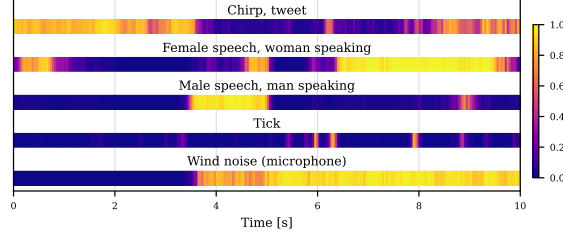
Results. Table 13 presents the results across the different SED test sets, grouped into open-vocabulary and closed-vocabulary categories. Overall, PE_A-Frame demonstrates strong performance, achieving the highest scores on all test sets in PSDS1_T, indicating superior capability in accurately detecting temporal boundaries of target sounds. In particular, PE_A-Frame attains the best performance on DESED across all metrics, highlighting its robustness in real-world acoustic environments, as DESED comprises real recordings with fine-grained human annotations [89]. As expected, PretrainedSED performs well on AudioSet-Strong, as it is optimized for that specific ontology; however, its closed-vocabulary nature prevents its application to the other test sets. Finally, FLAM performs best on UrbanSED, which is a synthetic and relatively unrealistic dataset. We hypothesize that this is because, unlike our model, their system was also trained on UrbanSED, giving it an inherent advantage on this benchmark. Moreover, FLAM operates with a coarser frame rate of 3.2 Hz, which limits its ability to perform fine-grained temporal detection and may lead to lower performance on intersection-based metrics.



(a) Input spectrogram



(b) Annotated “ground-truth” labels



(c) Predicted scores

Table 12 Sound event detection example using PE_A-Frame. The model successfully detects all sound events, accurately distinguishing between male and female speech, and capturing short transient events such as “Tick” enabled by its high temporal resolution (25 Hz).

	Open-vocabulary SED				Closed-vocabulary SED						UrbanSED (10 classes)			
	Internal Bench		ASFX-SED		AudioSet-Strong (407 classes)			DESED (10 classes)			UrbanSED (10 classes)			
	AUROC	AUROC	AUROC	AUROC	PSDS1 _A	PSDS1 _T	AUROC	PSDS1 _A	PSDS1 _T	AUROC	PSDS1 _A	PSDS1 _T	AUROC	
PE_A-Frame L	0.91	0.83	0.43	0.61	0.96	0.34	0.58	0.97	0.12	0.22	0.89			
PE_A-Frame B	0.92	0.83	0.42	0.60	0.96	0.39	0.56	0.98	0.12	0.21	0.89			
PE_A-Frame S	0.91	0.83	0.39	0.59	0.96	0.32	0.54	0.96	0.09	0.19	0.88			
PE_A-Frame B (from scratch)	0.89	0.76	0.22	0.55	0.89	0.10	0.52	0.89	0.01	0.08	0.82			

Table 14 Ablation results for model sizes small (S), base (B), large (L), and a base model trained from scratch. Larger models give only slight gains, while training from scratch leads to a substantial drop, highlighting the importance of large-scale pretraining.

5.1 Ablations studies for PE_{A-Frame}

Figure 12 presents an ablation study on the sampling probability p_{local} , which controls the ratio between the local-activity and the global-activity objective (see §3), conducted with the base model trained for 10k steps. We observe that higher values of p_{local} lead to improved PSDS_T scores, emphasizing that the local-activity loss benefits the detection of target sounds under the intersection-based evaluation metric. However, this comes at the cost of reduced PSDS_A, which penalizes false positives that may arise because the model contrasts fewer non-target sound events and instead focuses more narrowly on local alignment. Furthermore, we observe a monotonic increase in AUROC on the internal benchmark and an increase up to $p_{\text{local}} = 0.8$ on the ASFX-SED benchmark, followed by a drop thereafter. A value of $p_{\text{local}} = 0.7$ provides a favorable trade-off between these metrics, and we therefore adopt it as the default setting in all subsequent experiments.

An optimal value of p_{local} ultimately depends on the intended application of the SED system. If the goal is to precisely detect sound event boundaries for a given set of target events, it is recommended to use a higher p_{local} value. Conversely, if the application prioritizes minimizing false positives, such as in continuous environmental monitoring or safety-critical detection scenarios (e.g., false alarms in smart home or surveillance systems), a lower p_{local} may be more favorable.

Table 14 reports ablation results for different model sizes (large, base, and small), and the base model trained from scratch without pretrained weights. The results show that larger models yield only a slight improvement in performance metrics. However, there is a notable drop when the model is trained from scratch, highlighting the importance of large-scale pretraining for achieving strong performance.

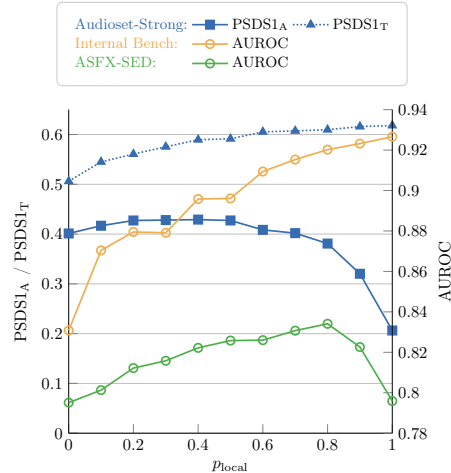


Figure 12 Effect of local-activity sampling. p_{local} trades off local vs. global activity, with $p_{\text{local}} = 0.7$ giving the best balance between PSDS_T, PSDS_A, and AUROC.

6 Summary

We have presented PE_{AV}, a family of audio-video-text encoders trained with contrastive objectives that jointly align information across all modalities at scale. Our audiovisual data engine expands data scale and diversity, and produces high-quality synthetic captions that outperform weak audio captioners while being complementary to real captions. Using this large-scale and diverse data, we scaled the contrastive objective to ten cross-modal pairs, yielding unified audio-video-text representations for perception. Our resulting unified embeddings achieved state-of-the-art zero-shot performance on a broad suite of benchmarks. Our audio encoder shows broad coverage across sound, speech, and music domains. Given the strong performance of PE_{AV}, we hope that the community builds upon it as a foundation for future work in omni-modal perception and generation.

7 Acknowledgement

We would like to thank Yi-Chiao Wu, Andros Tjandra, Bowen Shi, Dangna Li, Peng-Jen Chen, Robin San Roman, Helin Wang, Carleigh Wood, Andrew Westbury, Vanessa Stark, George Orlin, Anushka Sagar, Vivian Lee, Josh Terry, Helen Klein, Mallika Malhotra, Ty Toledano, Cynthia Gao, Ana Laraia, Mitesh Kumar Singh, John Hoffmann, Andrea Madotto, Muhammad Maaz, Shuming Hu, Daniel Bolya, Vincent Cho, Jianwei Yang, Rafael Valle, Manohar Paluri, Parth Malani, Natacha Supper, Amit Gala, Kyle Bendsen, for their inspiring discussions and timely support throughout this work.

Appendix

A Overview

The Appendix is organized as follows. We first discuss the related work in §B. Then we provide the details of building PE-AV’s audiovisual data engine and the stage-1 and stage-2 prompts used for generating synthetic captions in §C. Next, in §D, we provide additional implementation details of PE-AV including the full hyperparameter setup, training recipe (§D.1), and an efficient implementation (§D.2) to expand sigmoid contrastive loss for audio-video-text training. We also provide more details for our evaluation protocol to ensure reproducibility in §D.3. Finally, we present additional experiments in §E.

B Related Work

Learning visual, acoustic, and textual representations has become central to building multimodal foundation models for perception. By aligning images, video, audio, and language in a shared embedding space, contrastive vision–language and audio–language encoders enable strong zero-shot performance across diverse benchmarks: zero-shot audio retrieval on AudioCaps [27, 94, 96], zero-shot image classification on ImageNet [23], and zero-shot text-to-video retrieval [42, 73, 79] on MSR-VTT [101]. Furthermore, these encoders now serve as critical perception front-ends for multi-modal large language models (MLLMs) [5, 6, 57, 60, 69, 85, 102].

Vision-Language Representation Learning. Vision–language contrastive pretraining was established by early works such as Virtex [24], ICMLM [77], and ConViRT [109], and later scaled up by CLIP [42, 73] and ALIGN [43] on significantly larger datasets and models.

Subsequently, a series of open-weight contrastive models [30, 52, 79, 84, 100, 108] have been developed to enhance CLIP’s performance and robustness. Notably, SigLIP [108] replaces softmax with a sigmoid objective, and FLIP [54] employs masking to accelerate training. Additionally, researchers have explored incorporating auxiliary objectives, such self-supervised losses [44, 63, 64] and captioning losses [86, 92, 106]. In the data part, a series of works [30, 31, 79, 100] have studied large-scale sourcing and filtering of web data. These efforts aim to boost model performance by scaling high-quality data through efficient data curation strategies. To further improve alignment and reduce noise in web-crawled data, several works [29, 50, 65, 99] explore re-captioning training images using MLLMs or VLMs. This strategy seeks to enhance text quality, thereby strengthening the robustness of the learned representations.

Recently, Perception Encoder (PE) [8] modernizes CLIP-style training and, with the Perception Language Model (PLM) [22] as a video data engine, scales image–video–language pretraining. Building upon PE and PLM, in this work, we further extend PE to build PE_{AV}, an audio-video-text encoder by incorporating the audio modality through model and data scaling with an audio-video data engine.

Audio/Speech Representation Learning. Self-supervised learning (SSL) has become a dominant approach for audio representation learning, leveraging large amounts of unlabeled data. Notable models for speech representation include wav2vec 2.0 [3], HuBERT [38], and WavLM [15]. SSAST [34], Audio-MAE [39], data2vec [4], and BEATs [16] were developed for general audio. Moreover, MERT [55] and MuQ [112] have advanced music-domain audio representations. Recent advancements aim to learn audio representations at lower cost [19, 56] or across multiple domains within a single model [12]. However, these methods are limited to single-modality learning and do not use cross-modal information.

Recently, there has also been growing interest in leveraging paired audio–text data to better align audio and text modalities. Inspired by the success of CLIP in vision–language learning, CLAP [27] introduced a contrastive language–audio pre-training objective; subsequent work such as LAION-CLAP [96], M2D-CLAP [67], FLAP [105], and AF-CLAP [32] scaled this paradigm to more data, added SSL objectives, and incorporated synthetic captions, yielding stronger and more transferable audio encoders (including for LLMs).

Toward Unified Audio-Video-Text Encoders. To move beyond audio-only or audio-text alignment, several works exploit the video modality to learn audiovisual representations. CAV-MAE [35] and MAViL [40] use video as complementary supervision and show strong results on classification and cross-modal retrieval. More recent “hub-style” approaches such as ImageBind [33], LanguageBind [111], and InternVid 2 [94] connect multiple modalities via a single anchor (image or language), but still suffer from scale mismatches between modality-pair datasets, which can hurt less-represented modalities, especially non-speech audio. In contrast, PE_{AV} focuses on large-scale, language-guided audiovisual representation learning by utilizing a robust audio-video data engine. This enables broader coverage of contrastive objectives, facilitating the learning of more robust audiovisual and text representations.

Sound Event Detection. Traditional SED systems operate under a closed-vocabulary setting, targeting a predefined and limited set of sound classes, where each class is assigned a binary label at every time frame [62]. The performance of SED models has improved considerably on small-scale datasets centered on domestic environments [41, 80, 89]. More recently, self-supervised learning (SSL) and large-scale pretraining of audio spectrogram transformers have dramatically advanced SED capabilities, enabling the detection of diverse and complex acoustic scenes across hundreds of sound categories [53, 78]. These developments mark a significant shift from traditional, closed-vocabulary SED to flexible, open-vocabulary paradigms [36, 98], which aim to identify the temporal boundaries of any sound event described by natural language.

C Audio-Video Data Engine

In the following, we provide details of the prompts and examples for the stage-1 and stage-2 pipelines used to generate audio, video, and audiovisual captions using the audio-video data engine.

C.1 Stage-1 Prompts

The stage-1 prompt used in the data engine is as follows. We leverage CoNeTTe [49] and ENCLAP [47], as well as an internal video captioner.

LLM Prompts for Visual Captions

Create primarily visual captions that focus on what can be seen in the video. Video captions are your reliable source - **ALWAYS** create a caption from them, even if audio doesn't match. Handle repetitive video descriptions by summarizing while preserving all unique details. Audio can optionally enhance but should never drive the caption. Remember: (1) NEVER output an empty caption (2) **ALWAYS** create a caption from video content (3) If audio doesn't match, use only video details

Video Caption Principles

- **Primary Source:** **ALWAYS** use video captions
- **Detail Preservation:** Keep all distinct visual elements
- **Redundancy:** Clean up repetitive descriptions
- **Flow:** Create natural, coherent sentences

Required Output

- Video summary (clean, non-repetitive)
- Audio context (if used)
- Visual-focused caption between <BOS> and <EOS>
- Explanation of choices

Example 1

Input: INPUT FOR AUDIO-VISUAL:

- **VIDEO CAPTIONS:**
 - A professional surfer in a black wetsuit performs an aerial maneuver on a bright red surfboard against massive white waves.
 - An experienced surfer wearing dark gear rides along the crest of a towering ocean wave on their red board.
 - A skilled surfer executes a 360-degree turn while surfing on crystal clear blue waters.
- **AUDIO CAPTIONS (WITH CONFIDENCE LABELS):**
 - The thunderous crash of ocean waves fills the air. [confidence: HIGH_CONF]
 - Cat and dog meowing. [confidence: LOW_CONF]

Main Goal: Create a primarily visual caption that focuses on what can be seen in the video.

Video Caption Handling:

- Video captions are your primary and reliable source - **ALWAYS** use them
- Preserve all distinct visual details (colors, actions, numbers, descriptions)
- If video captions are repetitive, summarize while keeping all unique details
- Combine multiple video perspectives into natural-flowing sentences

Audio Caption Handling (Optional):

- Audio is strictly optional - visual details should stand alone
- Only consider HIGH_CONF audio that directly matches video content
- When using audio, add it at the end of the caption without disrupting visual flow

Output:

- Video summary: A professional surfer in a black wetsuit performs aerial maneuvers and a 360-degree turn on a bright red surfboard, riding along the crest of towering white waves in crystal clear blue waters.
- Audio summary: Wave sounds [HIGH_CONF] align with visible wave activity.
- Merged caption: <BOS> A professional surfer in a black wetsuit executes impressive aerial maneuvers and a 360-degree turn on their bright red surfboard, riding along the crest of towering white waves in crystal clear blue waters. <EOS>
- Explanation: Focused on rich visual details (wetsuit color, specific moves, board color, wave description). Though wave sounds matched, kept focus on visual elements.

LLM Prompts for Rewriting Audio Captions

Your task is to generate an **audio-focused caption** from model-generated video and audio captions for the same audio-visual input. All video captions are equally likely to be correct. Audio captions are generated using only audio, and different objects can produce similar sounds (e.g., machine low hum can be confused with crickets, lawn mower cutting grass may sound similar to engine whirring). Sometimes the video and audio may not correspond to each other as the recorded object may be far away. Consider if the described sounds are plausible given the video context. Each audio caption has a confidence label: **LOW_CONF**, **MED_CONF**, or **HIGH_CONF**: **LOW_CONF**: This caption is likely incorrect; when only **LOW_CONF** captions are present, use details that align with video. **MED_CONF**: At least one sound in the caption is correct; others may be incorrect. Only use details aligned with the video. **HIGH_CONF**: Generally reliable caption. Include all information with minor video-based adjustments. Prioritize over video caption if clear conflict. Your task is to merge the video and audio captions into a single caption, focusing on details determinable from audio. Summarize redundant captions before merging. If captions conflict, favor **HIGH_CONF** audio after verifying plausibility. When only **LOW_CONF** captions exist, try using common elements with video to create an audio-focused summary with general details.

Steps

1. Summarize the video captions.
2. Identify the audio captions relevant to the video scene and summarize them (dropping irrelevant ones). Verify **HIGH_CONF** details from given video context.
3. Merge the summarized captions into a single caption, focusing on plausible audio-based details, ignoring non-audio details like color.

Keep your answer succinct. Provide: (1) Summarized video caption. (2) Summarized audio caption. Include all plausible **HIGH_CONF** details. (3) A final merged caption enclosed between **<BOS>** and **<EOS>**.

Example 1

Input: INPUT FOR AUDIO-VISUAL:

- VIDEO CAPTIONS:
 - A person surfing in the clear blue ocean in front of the large white waves.
 - A tan man is surfing in the middle of the vast ocean and it starts to wave in the ocean.
 - A surfer on a bright red surfboard rides in a towering wave, then jumps up and starts surfing.
- AUDIO CAPTIONS (WITH CONFIDENCE LABELS):
 - The ocean waves can be heard. [confidence: **HIGH_CONF**]
 - Men talking. [confidence: **HIGH_CONF**]

YOUR TASK:

- Write an audio-focused summary caption.
- Summarize redundant or incomplete captions, focusing on details determinable from audio alone, such as gender, species, or car model, while ignoring vision-specific details like colors.
- If audio captions conflict, prioritize **HIGH_CONF** captions and include details, even if they seem to conflict with video. Make adjustments only when video clearly suggests a more plausible sound source, as the audio source may be off-camera or far away.
- Ignore **LOW_CONF**.
- Include **MED_CONF** details that seem plausible given the video.
- If no captions remain, create a short summary from the video. Output empty merged caption like **<BOS><EOS>** when caption cannot be created.

Output:

- Video summary: A tan man is surfing in the clear blue ocean with a bright red surfboard in front of large white waves.
- Audio summary: Sounds of waves and men speaking are heard.
- Merged caption: **<BOS> A man is surfing in the ocean, riding large waves, accompanied by the sounds of waves and men speaking. <EOS>**
- Explanation: Combining 'ocean waves' from first audio caption and 'men talking' from second caption to summarize using both **HIGH_CONF**. Added large waves and man details using video caption in the merged caption.

LLM Prompts for Rewriting Audio-Video Captions

You are tasked with generating **comprehensive audio-visual captions** that effectively combine information from both modalities. You will receive model-generated video captions and audio captions, each audio caption having a confidence label: `LOW_CONF`, `MED_CONF`, or `HIGH_CONF`.

Key Guidelines

- **Video captions are generally reliable** – ALWAYS use video information.
- **Audio captions** are based on only audio, and different objects can produce similar sounds (e.g., lawn mower and car engine). For audio captions: (1) `HIGH_CONF`: Include if there's any plausible connection to the video context. (2) `MED_CONF`: Use only when clearly complementing video information. (3) `LOW_CONF`: Ignore these captions.
- When `HIGH_CONF` audio seems unrelated to video: (1) Include both video and audio information. (2) Add note that they might not correspond.
- Look for creative ways to interpret audio captions in the video context using generic terms.
- Be generous in finding plausible connections between modalities by using broader categories. For example: (1) If audio mentions specific vehicles (car/truck) and video shows any vehicle – use generic terms like vehicle/engine/sounds. (2) If audio describes water sounds and video shows any liquid – include it. (3) If audio mentions speaking/talking and video shows people – connect them.

For each input, provide:

- **Video summary:** Key visual elements and actions.
- **Audio summary:** Relevant sounds and speech from `HIGH_CONF` captions.
- **Merged caption:** Natural combination of both modalities between `<BOS>` and `<EOS>`.
- **Brief explanation** of your integration choices.

Remember: (1) NEVER output an empty caption. (2) ALWAYS include video information. (3) Be generous in finding plausible audio-video connections. (4) When using unrelated `HIGH_CONF` audio, note the potential mismatch.

Example 1

INPUT FOR AUDIO-VISUAL CAPTIONING:

- **VIDEO CAPTIONS:**
 - A drain on a tiled floor shows signs of clogging with debris.
 - The metallic drain cover is partially lifted, revealing dirty water inside.
 - The surrounding tiles appear stained and poorly maintained.
- **AUDIO CAPTIONS (WITH CONFIDENCE LABELS):**
 - Water is splashing with a scraping sound. [confidence: `HIGH_CONF`]
 - People are talking in a foreign language. [confidence: `HIGH_CONF`]

YOUR TASK:

- Always create a comprehensive caption using the video information as primary source.
- For audio captions:
 - Use `HIGH_CONF` audio captions that seem plausible given the video context.
 - Include `MED_CONF` details only when they clearly complement video information.
 - Ignore `LOW_CONF` audio captions.
- When video and `HIGH_CONF` audio seem unrelated:
 - Include both video and audio information.
 - Note that they might not correspond to each other.
- Never output an empty caption – always use at least the video information.
- Be generous in finding plausible connections between audio and video.

Output:

- Video summary: A clogged metallic drain on a tiled floor shows debris and dirty water with a partially lifted cover.
- Audio summary: Sounds of water splashing and scraping are heard.
- Merged caption: `<BOS>` A clogged drain on a tiled floor contains dirty water, with splashing and scraping sounds as the water moves through the debris. `<EOS>`
- Explanation: Combined visual details of the drain with relevant `HIGH_CONF` audio of water and scraping sounds, ignoring unrelated audio about people talking.

C.2 PLM-AV Training Details

In the warm-up phase we only train a MLP layer on 4M synthetic captions to project the audio-visual / audio embeddings to the same dimensions as LLM embeddings. In the mid-training phase, we fine-tune the entire model on a 30M synthetic captions previously described. In the final stage, we fine-tune on a curated mix of data focused on audio-visual QA, captioning, instrument recognition, sound tagging, and paralinguistic attributes. Our key goal is to have a model that can produce an audio caption in natural language, or produce a list of sound events in Noun-Verb format. We additionally focus on improving the understanding of the acoustic environment. In Tab. 15, we show the performance of the PLM-AV models when measured on held-out Audiocaps [46] and Clotho-V2 [25] datasets. We use CLAP score from LAION [96] model to measure the quality of audio captions. We find that even in out-of-domain settings the model produces CLAP scores in same ball-park as ground-truth captions.

C.3 Stage-2 Prompts

Stage-2: PLM Prompts for Fine-Grained Video Caption

Create a fine-grained caption of a video using the provided metadata (if applicable), video caption, and frame captions.

Task: Extract key information from the captions and combine it into an alt text format using single phrase or set of phrases that includes all relevant details.

Steps to Follow:

- Review the metadata if (title and description) for general context, you can rely it for entity names but do not rely on it as the primary source of information for your caption.
- Blend title / description with video caption and frame captions for the main storyline
- Extract the most relevant and concise information.
- Combine extracted information into a alt text format using short phrase or set of phrases with approximately 120 tokens, considering special characters like comma as part of the token count.
- Prioritize including all key information over sentence structure or grammar.
- Minimize the use of special characters and focus of key information.

What to Avoid:

- Avoid adding or inferring information not present in the original metadata and captions.
- Avoid using complex sentence structures or prioritizing sentence flow.

Create a concise caption with the full details of the video based on the metadata, video caption, and frame captions.

Stage-2: Final LLM Summarization Prompts for Stage-2 Video Captions

Task:

You are provided with two types of captions for the same video:

1. **Video-level captions:** A high-level summary of the entire video.
2. **Fine-grained captions:** Detailed descriptions of specific events within the video.

Goal:

Write a single, concise, and coherent summary that:

- Clearly captures the main events of the video.
- Preserves important actions, objects, and contextual information from both caption types.
- Avoids unnecessary repetition of frame-by-frame details.
- Resolves any inconsistencies by prioritizing the video-level caption, unless the fine-grained caption adds essential information.
- Is written as a single sentence, not exceeding 72 words.

Input Format:

- Video-level captions: <stage1_vcap>
- Fine-grained captions: <plm_vcap>

Output:

A single-sentence summary describing the video.

Dataset	Ground Truth	PLM-AV (NPVP)	PLM-AV (caption)
Audiocaps	0.52	0.54	0.46
Clotho-V2	0.57	0.34	0.54

Table 15 Performance comparison with ground-truth captions using CLAP scores from LAION-CLAP model on AudioCaps and Clotho-V2 datasets. We find that PLM-AV produces high quality tags and captions even on the out-of-domain datasets.

25

D Implementation Details

D.1 Architecture and Training Setups

Model Architecture. We provide the detailed parameters of PE_{AV} in Tab. 16. For the frame encoder, we utilize the pre-trained PE-L [8] ($\sim 320\text{M}$ parameters) as the base frame encoder to capture spatial context, and employ a video encoder on top of it to encode temporal context. By default video frames are sampled under 30 frames-per-second (fps) from up to 30 seconds videos. Each frame is transformed into 336×336 resolution and then encoded into one CLS token via PE-L . To capture temporal context across frames, we stack 4 additional shallow Transformer layers ($30\text{M} \sim 180\text{M}$ parameters) as the video encoder on top of the frame encoder outputs. Note that we choose to freeze the frame encoder in PE_{AV} to ensure comparable image-only performance as in PE-L .

For the audio modality, we pre-train a DAC-VAE with in-house audio data. We use it to encode raw audio into 25×128 -dimensional vectors for a 1-second audio clip (and 750×128 for a 30-second audio), which serve as input to PE_{AV} . For the random-projection quantization module in BEST-RQ, we first project DAC-VAE features to a 16-dimensional latent space and quantize these features with four codebooks, each consisting of 16384 codewords. The base audio encoder, PE_{AVB} , is composed of 16 Transformer layers with around 0.21B parameters, while the large variant, PE_{AVL} , contains 28 layers and 1.11B parameters. The small model PE_{AVS} contains 12 layers and 0.09B parameters. We scale the hidden dimension proportionally to the number of layers with a factor of 64, and adjust the number of heads with a factor of 0.5.

To integrate audio and video features, we interpolate the video and audio token sequences to the same sequence length for alignment, then concatenate them along the channel dimension. This combined representation is fed into the audio-visual fusion module, which comprises 6 Transformer layers designed to incorporate both audio and video context within the video. The hidden dimension of the fusion tower also scales with the number of layers in the audio encoder, using a factor of 64. For the text encoder, to extend our support to transcript data which requires long context length, instead of using paired text encoder in PE-L , we use pre-trained ModernBERT with 28 layers to accommodate input texts up to 512 tokens. Based on early experiments, we use the 22nd-layer output, and we keep the text tower unfrozen during training.

We employ customized Transformer configurations as detailed in Tab. 16. For pooling, we add an attention pooling block in the last-layer of video, audio, and audio-video Transformer. Regarding positional embedding, we use 2D RoPE [83] for relative positional embeddings. We additionally add a 2D learnable absolute positional embeddings (abs) the same size as the model’s input resolution for the frame encoder. Finally, for simplicity, we use an input mean and standard deviation of $(0.5, 0.5, 0.5)$.

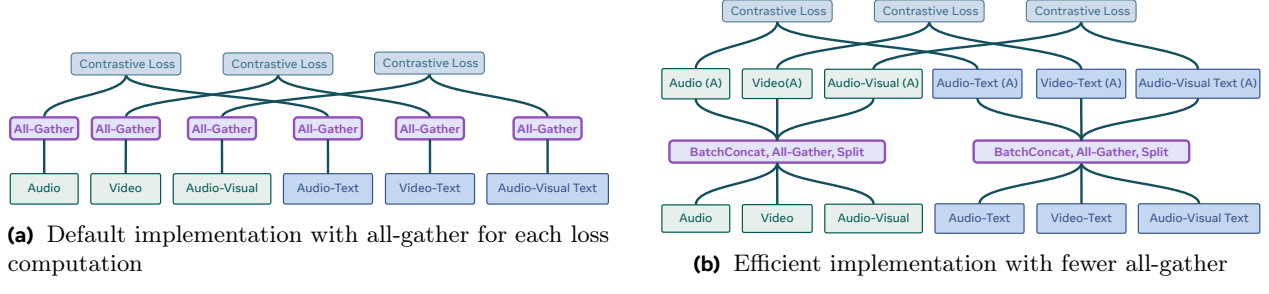
Scale	Tower	Params	Width	Depth	MLP	Heads	CLIP Dim	Pooling	Positional Embedding	Resolution & Context Len	Patch Size
S	Audio	0.09B	768	12	2048	6	1024	Attn Pool	RoPE	-	-
	Frame (PE-L)	0.32B	1024	24	4096	16	-	Attn Pool	RoPE+Abs	336	14
	Vision (Temporal)	0.03B	768	4	2048	6	1024	Attn Pool	RoPE	-	-
	Audio-Video	0.05B	768	6	2048	6	1024	Attn Pool	RoPE	-	-
B	Text	0.39B	1024	28	5248	16	1024	First Token	RoPE	512	-
	Audio	0.21B	1024	16	2752	8	1024	Attn Pool	RoPE	-	-
	Frame (PE-L)	0.32B	1024	24	4096	16	-	Attn Pool	RoPE+Abs	336	14
	Vision (Temporal)	0.06B	1024	4	2752	8	1024	Attn Pool	RoPE	-	-
L	Audio-Video	0.08B	1024	6	2752	8	1024	Attn Pool	RoPE	-	-
	Text	0.39B	1024	28	5248	16	1024	First Token	RoPE	512	-
	Audio	1.11B	1792	28	4800	14	1024	Attn Pool	RoPE	-	-
	Frame (PE-L)	0.32B	1024	24	4096	16	-	Attn Pool	RoPE+Abs	336	14
L	Vision (Temporal)	0.18B	1792	4	4800	14	1024	Attn Pool	RoPE	-	-
	Audio-Video	0.25B	1792	6	4800	14	1024	Attn Pool	RoPE	-	-
	Text	0.39B	1024	28	5248	16	1024	First Token	RoPE	512	-

Table 16 PE_{AV} Model Configurations.

D.2 Efficient Scaling of Contrastive Pairs

Fig. 13 sketches our efficient implementation for contrastive loss scaling. The default strategy performs two `all_gather` operations for every loss pair, so with P pairs the step performs $2P$ collectives. As node count grows, the all gather operations dominate runtime.

In our efficient implementation, we *reduce the number of all gather calls to two* irrespective of the number of loss pairs involved. We stack the first and second arguments of all P pairs along the batch dimension. We then issue a single `all_gather` over the stacked tensors to collect all modalities, and then split the result using recorded batch sizes before evaluating each loss.



(a) Default implementation with all-gather for each loss computation

(b) Efficient implementation with fewer all-gather

Figure 13 Efficient implementation for SigLIP scaling. *Left:* Naïve computation involves **two `all_gather`** calls per loss term which makes it hard to scale as the number of loss terms increase. *Right:* Our approach concatenates the first terms across all pairs along the batch axis (and likewise for the second terms), performs a **single `all_gather`** independent of the number of pairs, then splits by batch sizes before computing losses. This reduces collectives and improves throughput; in our setup (4 pairs, 8 nodes) we observe $\sim 40\text{--}50\%$ speedup.

Batch-wise concat/split is far cheaper than multiple cross-node collectives, yielding fewer synchronizations and better bandwidth utilization; in practice (4 pairs, 8 nodes) this reduces step time by approximately 40–50%.

Training Recipe As discussed in §2 in the Main text, the training of PE_{AV} involves two stages: 1) audio-video pre-training; 2) video and speech fine-tuning. These two stages work together to develop a robust and effective PE_{AV} model. We first provide the complete training recipes for 1) audio-video pre-training in Tab. 17 and 2) video and speech fine-tuning in Tab. 18.

config	values
optimizer	AdamW
β_1, β_2	(0.9, 0.999)
weight decay	0.0
learning rate	1e-4
batch size	3024
warm-up steps	500
training steps	250K
data quantity	92M
samples seen	750M

Table 17 Detailed Pre-training Setup.

Table 18 Detailed Fine-tuning Setup.

Table 19 Detailed Ablation Setup.

D.3 Zero-Shot Classification and Retrieval

Zero-Shot Evaluation on Images and Videos. We use CLIPBench² for zero-shot classification and retrieval benchmarking. The benchmark datasets and splits are obtained from the original dataset websites or HuggingFace. We extend zero-shot classification and retrieval in CLIPBench to include additional audio and video datasets such as AudioCaps, MSR-VTT, and Kinetics. We release our model checkpoints, evaluation code, and scripts for reproducibility.

Prompt Design. For zero-shot video-text retrieval, we rely solely on the original captions without any additional prompts. In contrast, for zero-shot classification, we utilize task-specific prompts graciously provided by the InternVL [20] authors. All additional dataset-specific prompts are released for reproducibility. For example, we employ specific prompts for zero-shot video classification on Kinetics datasets (e.g., K400, K600, K700).

²https://github.com/LAION-AI/CLIP_benchmark

Zero-Shot Video Classification Prompts - Kinetics

a photo of {c}. a photo of a person {c}. a photo of a person using {c}. a photo of a person doing {c}. a photo of a person during {c}. a photo of a person performing {c}. a photo of a person practicing {c}. a video of {c}. a video of a person {c}. a video of a person using {c}. a video of a person doing {c}. a video of a person during {c}. a video of a person performing {c}. a video of a person practicing {c}. a example of {c}. a example of a person {c}. a example of a person using {c}. a example of a person doing {c}. a example of a person during {c}. a example of a person performing {c}. a example of a person practicing {c}. a demonstration of {c}. a demonstration of a person {c}. a demonstration of a person using {c}. a demonstration of a person doing {c}. a demonstration of a person during {c}. a demonstration of a person performing {c}. a demonstration of a person practicing {c}.

Evaluation Method. For all the zero-shot evaluation, we follow [20] in using *retrieval reweighting* (DSL) to apply normalization over the softmax score distribution to the similarities used for retrieval:

$$\text{sims} = \text{sims} * \text{softmax}(\text{sims}, \text{dim}=0) \quad (5)$$

This slightly improves retrieval for most models, so we do it for all models we evaluate for fairness. Notably, we were able to reproduce the reported numbers for most papers with these techniques, but for cases where we could not, we default to the reported number.

For all retrieval tasks, we use dual-softmax [21] for both our models and other baselines. Empirically, we find that sharpening the final logits by a factor of 10 improves downstream performance. This adjustment aligns with the intuition that the model was trained with a scaled logit space to classify paired samples effectively. We also ignore the bias term, as it does not affect relative rankings and softmax is invariant to additive shifts.

E Additional Experimental Results

In this section, we provide the complete benchmark results for the data ablation in Tab. 20 (data engine), Tab. 7 (real vs synthetic data), and Tab. 22 (data scaling). The complete model scaling results are shown in Tab. 23 and for contrastive loss in Tab. 24.

Additionally, we include additional ablation studies on (1) choice of the text encoder; (2) impact of video frame rate; and (3) BEST-RQ loss in audio encoder training. Moreover, we provide extensive retrieval results of Tab. 2-3, and joint-modal results of Tab. 4 in the main paper.

Caption Type	Sound-Retrieval						Sound-Classification						Speech-Classification						Video-Retrieval				Video-Classification													
	AudioCaps		VALOR		Internal		VGGSound		GTzan		Cremad		CV-13		D-SUPERB			VTT		MSVD		ANet		K400		K700		HMDB								
	T → A	A → V	T → AV	A → V	T → A	A → V	A → T	AV → T	A → T	A → T	A → T	A → T	accent	lid	emo	vocal	T → V	T → V	T → V	T → V	V → T	V → T	V → T	V → T	V → T	V → T										
EnCLAP	23.7	30.8	56.8	24.0	20.3	19.8	50.5	35.9	10.9	24.0	40.0	57.1	31.3	47.1	55.1	49.1	38.0	44.7	26.8	36.1	59.6	24.4	25.2	29.3	55.6	28.8	12.2	21.5	30.8	67.4	31.1	49.2	56.8	49.5	38.7	46.4
CoNeTTE	30.3	31.6	62.1	22.6	28.4	39.3	57.2	38.4	15.1	21.5	32.1	61.3	36.2	53.7	56.8	56.6	44.9	49.1	32.2	32.0	64.6	25.2	29.7	44.3	59.8	32.8	16.8	30.0	34.2	73.6	36.2	53.9	57.7	55.8	45.3	51.1
Stage-1																																				
Stage-2																																				

Table 20 Data Engine. Compared to off-the-shelf captioners (EnCLAP [47] and CoNeTTE [49]), the proposed data engine significantly improves the data quality by taking into account video context and confidence score.

Real Data	Syn. Data	Sound-Retrieval						Sound-Classification						Speech-Classification						Video-Retrieval				Video-Classification															
		AudioCaps		VALOR		Internal		VGGSound		GTzan		Cremad		CV-13		D-SUPERB			VTT		MSVD		ANet		K400		K700		HMDB										
		T → A	A → V	T → AV	A → V	A → T	AV → T	A → T	A → T	A → T	A → T	A → T	accent	lid	emo	vocal	T → V	T → V	T → V	T → V	V → T	V → T	V → T	V → T	V → T	V → T	V → T												
0x	1x	26.1	39.1	58.4	31.0	30.2	44.3	60.7	28.2	18.1	37.5	15.0	69.7	32.7	47.1	55.4	68.4	57.2	55.4	1x	16.4	28.1	0.0	1.7	18.3	25.5	58.4	31.1	11.3	20.5	27.9	54.6	0.1	0.3	0.0	0.3	1.4		
1x	0x	27.1	34.9	53.7	14.4	25.2	27.3	41.3	65.1	28.8	18.5	36.0	25.4	64.9	29.8	46.7	42.3	63.7	51.4	52.8	10x	32.5	44.3	63.2	25.2	31.9	44.8	62.0	30.7	23.5	46.0	37.5	74.2	32.8	47.8	53.8	66.4	54.9	58.2
1x	20x	30.6	42.9	63.7	26.5	31.2	44.4	63.0	31.3	16.8	43.0	23.8	77.1	47.2	56.1	63.6	52.6	51.5	30x	30.8	43.6	60.5	29.0	30.4	43.1	58.9	30.2	23.1	51.0	30.4	75.6	33.8	46.9	55.1	61.7	50.3	51.3		

Table 21 Comparing different mixing ratios of real and synthetic caption data. Mixing both data types outperforms using only real or synthetic data. Higher synthetic ratios (till 1:10) further boost performance by improving diversity.

Text encoder. In Tab. 25, we present an ablation of different choices of text encoders for PE_{AV} with PE-L as the default visual encoder. We compare the performance of ModernBERT [95] with the original paired CLIP text encoder from PE-L [8]. After audio-video-text pre-training, we observe that the original PE-L text encoder performs better on video-centric tasks such as VTT [101] and Kinetics [45]. However, its performance lags on out-of-visual-domain concepts, such as audio events, in audio-focused tasks like text-to-audio retrieval in AudioCaps [46], and LID, emotion, vocal classification in Dynamic-SUPERB [107], where ModernBERT

Data Scale	Sound-Retrieval					Sound-Classification					Speech-Classification					Video-Retrieval			Video-Classification			
	AudioCaps		VALOR		Internal	VGGSound		GTzan		Cremad	CV-13		D-SUPERB			VTT		MSVD	ANet	K400	K700	HMDB
	T→A	A→V	T→AV	A→V	A→T	AV→T	A→T	AV→T	A→T	A→T	CV-13	lid	emo	vocal	T→V	T→V	T→V	V→T	V→T	V→T	V→T	
$\mathcal{O}(2M)$	27.0	38.1	57.8	18.1	27.4	40.4	60.2	30.6	20.2	36.0	32.9	66.3	32.8	47.6	50.4	48.0	36.9	41.6				
$\mathcal{O}(4M)$	29.6	46.1	64.6	22.1	30.1	43.4	63.9	28.6	17.2	41.5	25.8	66.4	34.9	51.6	53.1	51.5	40.5	51.7				
$\mathcal{O}(8M)$	31.3	44.8	65.2	23.9	32.0	44.7	61.8	29.9	18.9	39.5	39.2	73.9	34.5	52.8	55.5	54.0	42.8	48.8				
$\mathcal{O}(16M)$	32.1	48.7	65.9	24.1	33.1	45.2	62.1	26.1	19.3	41.0	35.4	74.4	36.2	54.0	56.5	54.2	43.0	50.3				
$\mathcal{O}(32M)$	32.8	50.6	67.5	23.7	32.9	45.4	62.0	27.9	18.1	39.0	30.4	76.5	35.6	53.7	56.5	55.8	43.7	51.9				
$\mathcal{O}(64M)$	33.6	47.0	67.0	26.2	34.3	46.2	63.8	33.3	16.0	43.0	24.2	71.8	35.6	53.7	57.7	55.1	43.9	50.7				

Table 22 Comparing performance as synthetic-caption data scale increases. Performance increases with synthetic-caption data scale (peaking at 64M), underscoring the value of diverse set of audio-visual-text data.

A-layers	A-params	V-params	Sound-Retrieval					Sound-Classification					Speech-Classification					Video-Retrieval			Video-Classification			
			AudioCaps		VALOR		Internal	VGGSound		GTzan		Cremad	CV-13		D-SUPERB			VTT		MSVD	ANet	K400	K700	HMDB
			T→A	A→V	T→AV	A→V	A→T	AV→T	A→T	AV→T	A→T	A→T	CV-13	lid	emo	vocal	T→V	T→V	T→V	T→V	V→T	V→T	V→T	
8	0.03B	0.34B	29.5	38.3	67.1	16.6	28.7	45.0	58.0	28.4	19.3	32.0	26.7	70.7	35.8	54.1	54.9	55.3	44.1	51.2				
12	0.09B	0.35B	32.0	46.0	67.8	23.1	31.4	45.4	63.1	27.9	21.9	38.0	35.4	72.2	36.6	54.0	56.3	55.7	44.5	51.6				
16	0.21B	0.38B	33.2	48.4	68.1	25.6	33.3	45.4	61.8	32.0	19.3	41.0	32.9	73.5	36.6	53.7	56.3	55.2	43.6	48.9				
20	0.41B	0.42B	34.4	57.2	67.9	27.3	33.6	46.2	62.8	35.9	21.9	44.0	31.7	74.0	37.3	53.2	56.7	56.0	44.6	52.4				
24	0.70B	0.45B	34.4	53.4	66.9	24.4	33.2	45.7	62.6	30.1	22.7	38.0	35.8	76.9	35.2	53.3	55.7	54.4	43.7	50.1				
28	1.11B	0.50B	34.3	56.7	66.6	24.7	34.2	44.9	65.0	32.7	16.0	34.0	32.5	78.1	35.5	53.3	56.7	53.3	43.0	49.0				

Table 23 Scaling the audio encoder. Scaling from 0.03B to 1.11B parameters shows consistent performance gains with depth. The observed saturation around 20 layers is likely due to limited training steps and data in the ablation setup.

Loss	A-V	A-AT	V-VT	V-AT	AV-VT	AV-AT	AV-AT	Sound-Retrieval					Sound-Classification					Speech-Classification					Video-Retrieval			Video-Classification			
								AudioCaps		VALOR		Internal	VGGSound		GTzan		Cremad	CV-13		D-SUPERB			VTT		MSVD	ANet	K400	K700	HMDB
								T→A	A→V	T→AV	A→V	A→T	AV→T	A→V	A→T	AV→T	A→T	A→T	CV-13	lid	emo	vocal	T→V	T→V	T→V	T→V	V→T	V→T	V→T
SigLIP	-	✓	-	-	-	-	-	31.9	0.1	0.0	0.0	32.4	0.5	60.4	30.8	23.5	52.5	30.4	76.1	0.1	0.2	0.0	0.3	0.1	2.2				
SigLIP	-	✓	-	-	✓	-	-	32.2	0.1	0.1	0.0	31.2	0.3	62.2	27.3	20.6	33.0	32.5	71.4	27.2	44.5	55.5	42.2	33.0	40.8				
SigLIP	-	✓	-	-	✓	-	-	33.0	0.0	47.1	0.1	31.9	0.3	56.6	30.6	18.1	36.0	32.1	71.8	26.1	42.5	53.0	41.8	31.3	42.1				
SigLIP	✓	✓	-	-	✓	-	-	31.9	45.6	47.5	24.7	30.6	0.4	53.3	25.2	21.9	38.5	32.1	70.0	27.3	44.2	47.0	39.7	30.1	36.4				
SigLIP	✓	✓	-	✓	✓	-	✓	31.4	49.5	66.3	25.1	32.5	45.1	61.0	26.2	18.1	43.5	32.5	76.5	34.5	53.9	56.7	55.8	43.8	49.7				
SigLIP	✓	✓	✓	✓	✓	✓	✓	32.9	45.7	68.3	21.8	33.3	45.5	62.4	33.2	17.2	47.5	30.4	74.7	33.9	54.1	57.2	54.2	43.1	48.9				

Table 24 Scaling the SigLIP objective. A: Audio, V: Video, AT: Audio text caption, VT: Video text caption. Expanding the contrastive objective to cover more modality pairs strengthens cross-modal alignment and improves zero-shot retrieval and classification. Audio-text-only training lags behind, while adding cross-modality pairs (e.g., V→AT, AV→VT) yields further gains. Performance peaks when the objective includes all eight pairs (bottom row).

Text Encoder	Sound-Retrieval					Sound-Classification					Speech-Classification					Video-Retrieval			Video-Classification			
	AudioCaps		VALOR		Internal	VGGSound		GTzan		Cremad	CV-13		D-SUPERB			VTT		MSVD	ANet	K400	K700	HMDB
	T→A	A→V	T→AV	A→V	A→T	AV→T	A→T	AV→T	A→T	A→T	CV-13	lid	emo	vocal	T→V	T→V	T→V	T→V	V→T	V→T	V→T	
PE-Text	30.5	49.1	66.6	23.1	33.3	47.3	62.1	25.9	19.3	46.5	23.3	59.7	45.3	60.4	52.2	66.7	57.6	55.3				
ModernBERT	34.1	49.0	66.5	25.3	34.1	46.1	63.0	29.5	18.1	47.0	37.9	74.2	36.2	53.3	57.4	54.6	44.0	50.2				

Table 25 Comparison of text encoder choices for PE_{AV} using the PE-L visual encoder. ModernBERT outperforms the original PE-L text encoder on audio-focused tasks due to its longer context (512 tokens vs. 32) and its support of general text domain, while PE-L performs better on video-centric tasks. As noted in main results, ModernBERT catches up with and surpasses the PE-L text encoder after fine-tuning, making it the preferred choice for PE_{AV}.

PT frames	FT frames	Sound-Retrieval					Sound-Classification					Speech-Classification					Video-Retrieval			Video-Classification			
		AudioCaps		VALOR		Internal	VGGSound		GTzan		Cremad	CV-13		D-SUPERB			VTT		MSVD	ANet	K400	K700	HMDB
		T→A	A→V	T→AV	A→V</																		

SSL Loss	Sound-Retrieval				Sound-Classification				Speech-Classification				Video-Retrieval		Video-Classification			
	AudioCaps		VALOR		Internal	VGGSound		GTzan	Cremad	CV-13	D-SUPERB		VTT	MSVD	ANet	K400	K700	HMDB
	T→A	A→V	T→AV	A→V	A→T	AV→T	A→T	A→T	accent	lid	emo	vocal	T→V	T→V	T→V	V→T	V→T	V→T
None	30.7	44.1	65.7	25.7	31.4	44.6	61.2	30.3	17.7	35.5	33.3	74.9	34.6	53.6	55.6	54.2	43.1	49.3
NCE	31.9	46.9	67.7	25.3	31.6	45.0	63.1	26.3	14.7	36.0	32.9	72.2	35.6	53.9	56.7	54.0	43.0	48.9
BEST-RQ	33.2	48.4	68.1	25.6	33.3	45.4	61.8	32.0	19.3	41.0	32.9	73.5	36.6	53.7	56.3	55.2	43.6	50.9

Table 27 Audio encoder losses: NCE vs. BEST-RQ. NCE follows wav2vec 2.0 contrastive objective using DAC-VAE features as negatives but skips quantization. BEST-RQ delivers the strongest results, outperforming NCE and no-SSL baselines. Speech and sound tasks benefit the most from the finer-grained representations encouraged by BEST-RQ.

training various models at both frame rates is computationally intensive, we performed this ablation with our largest model PE_{AVL}. We train for the full pre-training duration of 250K steps followed by 50K steps of fine-tuning, ensuring that conclusions are drawn from the strongest configuration.

For most tasks, models trained with these different frame rate configurations exhibit similar performance, while 30 FPS sampling provides a modest advantage, especially during the pre-training phase. However, models operating at higher frame rates achieve better results on downstream tasks that require fine-grained temporal understanding, such as ActivityNet and audio-video retrieval on the internal dataset with a wide duration variation. Notably, models trained with 30 FPS sampling inherently encode duration information, enabling them to retrieve audios or videos of similar length as the query. This also highlights a key limitation of existing audio-video retrieval benchmarks, which do not evaluate robustness to variation in duration. With this, for all other models, we adopt 30 FPS sampling during pre-training and later fine-tune with the same setup or with fixed 16-frame inputs.

BEST-RQ vs NCE Loss. In Tab. 27, we compare different SSL losses for the audio encoder. The NCE loss is similar to the contrastive loss in wav2vec 2.0, except that we skip the quantization step and use the DAC-VAE features as the negative samples directly. BEST-RQ offers the best overall results, significantly outperforming NCE loss and no SSL loss conditions. Video tasks retain performance while some even show slight improvement when the BEST-RQ loss is present. The results demonstrate the necessity of including BEST-RQ loss to enhance the performance of sound and speech tasks without compromising video capabilities, corroborating the hypothesis that encouraging fine-grained representations benefits speech-related tasks.

Table 28 Full Zero-Shot Retrieval Results. Per-dataset Recall@1 for all audio–text, video–text, and audio–video retrieval directions corresponding to the main audio and video tables. PE_{AV} consistently outperforms baseline models across most benchmarks and retrieval directions.

Model	Zero-Shot Retrieval												Zero-Shot Classification				
	AudioCaps $T \rightarrow A + V$	AudioCaps $T + A \rightarrow V$	AudioCaps $T + V \rightarrow A$	VALOR $T \rightarrow A + V$	VALOR $T + A \rightarrow V$	VALOR $T + V \rightarrow A$	VTT $T \rightarrow A + V$	VTT $T + A \rightarrow V$	VTT $T + V \rightarrow A$	VTT $T \rightarrow A + V$	VTT $T + V \rightarrow A$	VTT $T + A \rightarrow V$	DiDeMo $T \rightarrow A + V$	DiDeMo $T + A \rightarrow V$	DiDeMo $T + V \rightarrow A$	VGGSound $A \rightarrow T$	VGGSound $V \rightarrow T$
ImageBind [†] [33]	7.6	51.6	51.3	36.1	36.1	24.2	41.9	41.9	23.9	36.1	36.1	18.3	28.2	40.4	40.4		
LanguageBind [†] [111]	19.7	10.7	19.7	46.8	46.8	6.5	50.9	50.9	3.7	44.2	44.2	5.5	26.0	45.4	45.4		
PE _{AV} S-OOD [†]	40.2	76.6	75.3	69.8	69.8	57.7	52.0	64.0	65.3	53.7	55.2	55.5	40.0	46.3	46.3		
PE _{AV} S-OOD	36.8	73.0	89.1	76.1	88.8	65.2	48.3	86.7	63.9	48.0	76.2	51.4	40.0	46.3	52.5		
PE _{AV} B-OOD [†]	40.4	81.8	82.2	70.0	70.0	63.9	51.4	64.4	66.0	52.0	60.6	62.0	41.4	47.0	47.0		
PE _{AV} B-OOD	38.0	77.3	92.6	75.6	90.5	70.9	50.1	87.8	65.8	48.0	81.0	57.8	41.4	47.0	52.1		
PE _{AV} L-OOD [†]	43.4	87.5	86.1	70.2	72.2	73.1	51.5	70.0	71.6	52.7	66.8	67.7	43.9	46.7	46.7		
PE _{AV} L-OOD	38.7	82.9	93.3	76.0	92.0	77.2	49.9	89.0	69.8	48.8	82.1	62.1	43.9	46.7	52.0		
PE _{AV} S [†]	41.8	77.7	77.4	70.9	70.9	60.1	50.1	59.6	61.1	49.8	53.2	56.9	43.0	47.3	47.3		
PE _{AV} S	40.1	73.6	90.3	76.4	89.8	67.6	48.3	85.9	58.6	40.0	75.5	44.5	43.0	47.3	52.2		
PE _{AV} B [†]	42.7	83.5	83.7	71.2	71.2	65.3	50.1	62.3	63.8	49.6	61.6	63.4	44.5	47.8	47.8		
PE _{AV} B	41.0	79.9	93.2	76.9	91.1	72.0	48.1	86.3	60.2	39.8	80.7	51.9	44.5	47.8	52.7		
PE _{AV} L [†]	45.8	89.0	88.3	70.9	73.8	74.5	52.9	63.6	67.4	51.4	69.3	69.5	47.1	48.0	48.0		
PE _{AV} L	42.6	84.0	95.2	76.8	93.0	78.8	49.0	85.3	65.1	43.0	80.8	61.6	47.1	48.0	51.8		

Table 29 Zero-shot joint-modal retrieval and classification. For baselines and PE_{AV} variants marked with [†], joint queries are approximated via the max over unimodal results: $T + V \rightarrow A = \max(T \rightarrow A, V \rightarrow A)$, $T \rightarrow A + V = \max(T \rightarrow A, T \rightarrow V)$, and $T + A \rightarrow V = \max(T \rightarrow V, A \rightarrow V)$. All other PE_{AV} variants use native joint embeddings for $T + V$, $A + V$, and $T + A$. For all PE_{AV} models, we observe that joint embeddings are helpful when the input modalities are complimentary to each others. Specifically (i) for audio-only captions (*AudioCaps*) $V + T \rightarrow A$ significantly outperforms $V \rightarrow A$ and $T \rightarrow A$; (ii) for visual captions (*DiDeMo* & *MSR-VTT*) $A + T \rightarrow V$ improves over $A \rightarrow V$ and $T \rightarrow V$; (iii) for audio-visual captions (*VALOR*) both $V + T \rightarrow A$ and $A + T \rightarrow V$ help; (iv) *VGGSound*: $A + V \rightarrow T$ exceeds $A \rightarrow T$ and $V \rightarrow T$.

References

- [1] Lisa Anne Hendricks, Oliver Wang, Eli Shechtman, Josef Sivic, Trevor Darrell, and Bryan Russell. Localizing moments in video with natural language. In *Proceedings of the IEEE/CVF International Conference on Computer Vision (ICCV)*, 2017. [10](#), [12](#)
- [2] Rosana Ardila, Megan Branson, Kelly Davis, Michael Henretty, Michael Kohler, Josh Meyer, Reuben Morais, Lindsay Saunders, Francis M Tyers, and Gregor Weber. Common voice: A massively-multilingual speech corpus. *arXiv preprint arXiv:1912.06670*, 2019. [4](#), [11](#)
- [3] Alexei Baevski, Henry Zhou, Abdelrahman Mohamed, and Michael Auli. wav2vec 2.0: A framework for self-supervised learning of speech representations. In *Advances in Neural Information Processing Systems (NeurIPS) 33*, 2020. [20](#)
- [4] Alexei Baevski, Wei-Ning Hsu, Qiantong Xu, Arun Babu, Jiatao Gu, and Michael Auli. Data2vec: A general framework for self-supervised learning in speech, vision and language. In *International conference on machine learning*, pages 1298–1312. PMLR, 2022. [20](#)
- [5] Jinze Bai, Shuai Bai, Shusheng Yang, Shijie Wang, Sinan Tan, Peng Wang, Junyang Lin, Chang Zhou, and Jingren Zhou. Qwen-VL: A versatile vision-language model for understanding, localization, text reading, and beyond. *arXiv:2308.12966*, 2023. [20](#)
- [6] Lucas Beyer, Andreas Steiner, André Susano Pinto, Alexander Kolesnikov, Xiao Wang, Daniel Salz, Maxim Neumann, Ibrahim Alabdulmohsin, Michael Tschannen, Emanuele Bugliarello, Thomas Unterthiner, Daniel Keysers, Skanda Koppula, Fangyu Liu, Adam Grycner, Alexey A. Gritsenko, Neil Houlsby, Manoj Kumar, Keran Rong, Julian Eisenschlos, Rishabh Kabra, Matthias Bauer, Matko Bosnjak, Xi Chen, Matthias Minderer, Paul Voigtlaender, Ioana Bica, Ivana Balazevic, Joan Puigcerver, Pinelopi Papalampidi, Olivier J. Hénaff, Xi Xiong, Radu Soricut, Jeremiah Harmsen, and Xiaohua Zhai. PaliGemma: A versatile 3b VLM for transfer. *arXiv:2407.07726*, 2024. [20](#)
- [7] Çağdaş Bilen, Giacomo Ferroni, Francesco Tuveri, Juan Azcarreta, and Sacha Krstulović. A framework for the robust evaluation of sound event detection. In *ICASSP*, pages 61–65, 2020. [17](#)
- [8] Daniel Bolya, Po-Yao Huang, Peize Sun, Jang Hyun Cho, Andrea Madotto, Chen Wei, Tengyu Ma, Jiale Zhi, Jathushan Rajasegaran, Hanoona Rasheed, Junke Wang, Marco Monteiro, Hu Xu, Shiyu Dong, Nikhila Ravi, Daniel Li, Piotr Dollár, and Christoph Feichtenhofer. Perception encoder: The best visual embeddings are not at the output of the network. *arXiv:2504.13181*, 2025. [1](#), [2](#), [4](#), [5](#), [8](#), [10](#), [11](#), [12](#), [17](#), [20](#), [26](#), [28](#)

[9] Fabian Caba Heilbron, Victor Escorcia, Bernard Ghanem, and Juan Carlos Niebles. Activitynet: A large-scale video benchmark for human activity understanding. In *Proceedings of the IEEE Conference on Computer Vision and Pattern Recognition (CVPR)*, pages 961–970, 2015. [10](#), [12](#)

[10] H. Cao, D.G. Cooper, M.K. Keutmann, R.C. Gur, A. Nenkova, and R. Verma. Crema-d: Crowd-sourced emotional multimodal actors dataset. *IEEE Transactions on Affective Computing*, 5(4):377–390, 2014. [10](#), [11](#)

[11] Joao Carreira, Eric Noland, Chloe Banki-Horvath, Chloe Hillier, and Andrew Zisserman. A short note about kinetics-600/700. In *arXiv preprint arXiv:1907.06987*, 2019. [10](#)

[12] Heng-Jui Chang, Saurabhchand Bhati, James Glass, and Alexander H Liu. Usad: Universal speech and audio representation via distillation. In *IEEE Automatic Speech Recognition and Understanding Workshop (ASRU)*, 2025. [20](#)

[13] David L. Chen and William B. Dolan. Collecting highly parallel data for paraphrase evaluation. In *Proceedings of the 49th Annual Meeting of the Association for Computational Linguistics: Human Language Technologies*, pages 190–200, 2011. [10](#), [12](#)

[14] Honglie Chen, Weidi Xie, Andrea Vedaldi, and Andrew Zisserman. Vggsound: A large-scale audio-visual dataset. In *ICASSP 2020-2020 IEEE International Conference on Acoustics, Speech and Signal Processing (ICASSP)*, pages 721–725. IEEE, 2020. [10](#), [11](#), [12](#)

[15] Sanyuan Chen, Chengyi Wang, Zhengyang Chen, Yu Wu, Shujie Liu, Zhuo Chen, Jinyu Li, Naoyuki Kanda, Takuya Yoshioka, Xiong Xiao, et al. Wavlm: Large-scale self-supervised pre-training for full stack speech processing. *IEEE Journal of Selected Topics in Signal Processing*, 16(6):1505–1518, 2022. [20](#)

[16] Sanyuan Chen, Yu Wu, Chengyi Wang, Shujie Liu, Daniel Tompkins, Zhuo Chen, and Furu Wei. Beats: Audio pre-training with acoustic tokenizers. *arXiv preprint arXiv:2212.09058*, 2022. [20](#)

[17] Sihan Chen, Xingjian He, Longteng Guo, Xinxin Zhu, Weining Wang, Jinhui Tang, and Jing Liu. Valor: Vision-audio-language omni-perception pretraining model and dataset. *arXiv preprint arXiv:2304.08345*, 2023. [10](#), [11](#), [12](#)

[18] Sanyuan Chen, Yu Wu, Chengyi Wang, Shujie Liu, Daniel Tompkins, Zhuo Chen, Wanxiang Che, Xiangzhan Yu, and Furu Wei. BEATS: Audio pre-training with acoustic tokenizers. In *International Conference on Machine Learning*, pages 5178–5193, 2023. [18](#)

[19] Wenxi Chen, Yuzhe Liang, Ziyang Ma, Zhisheng Zheng, and Xie Chen. Eat: Self-supervised pre-training with efficient audio transformer. *arXiv preprint arXiv:2401.03497*, 2024. [20](#)

[20] Zhe Chen, Jiannan Wu, Wenhui Wang, Weijie Su, Guo Chen, Sen Xing, Muyan Zhong, Qinglong Zhang, Xizhou Zhu, Lewei Lu, Bin Li, Ping Luo, Tong Lu, Yu Qiao, and Jifeng Dai. InternVL: Scaling up vision foundation models and aligning for generic visual-linguistic tasks. In *CVPR*, 2024. [10](#), [12](#), [27](#), [28](#)

[21] Xing Cheng, Hezheng Lin, Xiangyu Wu, Fan Yang, and Dong Shen. Improving video-text retrieval by multi-stream corpus alignment and dual softmax loss. *arXiv preprint arXiv:2109.04290*, 2021. Version v3, Nov 2021. [10](#), [28](#)

[22] Jang Hyun Cho, Andrea Madotto, Effrosyni Mavroudi, Triantafyllos Afouras, Tushar Nagarajan, Muhammad Maaz, Yale Song, Tengyu Ma, Shuming Hu, Hanoona Rasheed, Peize Sun, Po-Yao Huang, Daniel Bolya, Suyog Jain, Miguel Martin, Huiyu Wang, Nikhila Ravi, Shashank Jain, Temmy Stark, Shane Moon, Babak Damavandi, Vivian Lee, Andrew Westbury, Salman Khan, Philipp Krähenbühl, Piotr Dollár, Lorenzo Torresani, Kristen Grauman, and Christoph Feichtenhofer. Perceptionlm: Open-access data and models for detailed visual understanding. *arXiv:2504.13180*, 2025. [4](#), [6](#), [8](#), [20](#)

[23] Jia Deng, Wei Dong, Richard Socher, Li-Jia Li, Kai Li, and Li Fei-Fei. ImageNet: A large-scale hierarchical image database. In *CVPR*, 2009. [20](#)

[24] Karan Desai and Justin Johnson. VirTex: Learning visual representations from textual annotations. In *CVPR*, 2021. [20](#)

[25] Konstantinos Drossos, Samuel Lipping, and Tuomas Virtanen. Clotho: an audio captioning dataset. In *ICASSP 2020 - 2020 IEEE International Conference on Acoustics, Speech and Signal Processing (ICASSP)*, pages 736–740, 2020. [10](#), [11](#), [25](#)

[26] Janek Ebbers, Reinhold Haeb-Umbach, and Romain Serizel. Threshold independent evaluation of sound event detection scores. In *ICASSP*, pages 1021–1025, 2022. [17](#)

[27] Benjamin Elizalde, Soham Deshmukh, Mahmoud Al Ismail, and Huaming Wang. CLAP: Learning audio concepts from natural language supervision. In *ICASSP 2023-2023 IEEE International Conference on Acoustics, Speech and Signal Processing (ICASSP)*, pages 1–5. IEEE, 2023. [2](#), [10](#), [11](#), [20](#), [30](#)

[28] Jesse Engel, Cinjon Resnick, Adam Roberts, Sander Dieleman, Douglas Eck, Karen Simonyan, and Mohammad Norouzi. Neural audio synthesis of musical notes with wavenet autoencoders. In *Proceedings of the 34th International Conference on Machine Learning (ICML)*, 2017. [10](#), [11](#)

[29] Lijie Fan, Dilip Krishnan, Phillip Isola, Dina Katabi, and Yonglong Tian. Improving CLIP training with language rewrites. In *NeurIPS*, 2023. [20](#)

[30] Alex Fang, Albin Madappally Jose, Amit Jain, Ludwig Schmidt, Alexander Toshev, and Vaishaal Shankar. Data filtering networks. In *ICLR*, 2024. [20](#)

[31] Samir Yitzhak Gadre, Gabriel Ilharco, Alex Fang, Jonathan Hayase, Georgios Smyrnis, Thao Nguyen, Ryan Marten, Mitchell Wortsman, Dhruba Ghosh, Jieyu Zhang, Eyal Orgad, Rahim Entezari, Giannis Daras, Sarah Pratt, Vivek Ramanujan, Yonatan Bitton, Kalyani Marathe, Stephen Mussmann, Richard Vencu, Mehdi Cherti, Ranjay Krishna, Pang Wei Koh, Olga Saukh, Alexander Ratner, Shuran Song, Hannaneh Hajishirzi, Ali Farhadi, Romain Beaumont, Sewoong Oh, Alex Dimakis, Jenia Jitsev, Yair Carmon, Vaishaal Shankar, and Ludwig Schmidt. DataComp: In search of the next generation of multimodal datasets. In *NeurIPS*, 2023. [20](#)

[32] Sreyan Ghosh, Zhifeng Kong, Sonal Kumar, S Sakshi, Jaehyeon Kim, Wei Ping, Rafael Valle, Dinesh Manocha, and Bryan Catanzaro. Audio Flamingo 2: An audio-language model with long-audio understanding and expert reasoning abilities. In *Forty-second International Conference on Machine Learning*, 2025. [2](#), [10](#), [11](#), [20](#), [30](#)

[33] Rohit Girdhar, Alaaeldin El-Nouby, Zhuang Liu, Mannat Singh, Kalyan Vasudev Alwala, Armand Joulin, and Ishan Misra. Imagebind: One embedding space to bind them all. In *Proceedings of the IEEE/CVF conference on computer vision and pattern recognition*, pages 15180–15190, 2023. [1](#), [2](#), [3](#), [10](#), [11](#), [12](#), [21](#), [30](#), [31](#)

[34] Yuan Gong, Cheng-I Lai, Yu-An Chung, and James Glass. Ssast: Self-supervised audio spectrogram transformer. In *Proceedings of the AAAI Conference on Artificial Intelligence*, pages 10699–10709, 2022. [20](#)

[35] Yuan Gong, Andrew Rouditchenko, Alexander H. Liu, David Harwath, Leonid Karlinsky, Hilde Kuehne, and James R. Glass. Contrastive audio-visual masked autoencoder. In *The Eleventh International Conference on Learning Representations*, 2023. [21](#)

[36] Jiarui Hai, Helin Wang, Weizhe Guo, and Mounya Elhilali. Flexsed: Towards open-vocabulary sound event detection. In *IEEE Workshop on Applications of Signal Processing to Audio and Acoustics (WASPAA)*, 2025. [17](#), [18](#), [21](#)

[37] Shawn Hershey, Daniel PW Ellis, Eduardo Fonseca, Aren Jansen, Caroline Liu, R Channing Moore, and Manoj Plakal. The benefit of temporally-strong labels in audio event classification. In *ICASSP*, pages 366–370, 2021. [17](#)

[38] Wei-Ning Hsu, Benjamin Bolte, Yao-Hung Hubert Tsai, Kushal Lakhotia, Ruslan Salakhutdinov, and Abdelrahman Mohamed. Hubert: Self-supervised speech representation learning by masked prediction of hidden units. *IEEE/ACM transactions on audio, speech, and language processing*, 29:3451–3460, 2021. [20](#)

[39] Po-Yao Huang, Hu Xu, Juncheng Li, Alexei Baevski, Michael Auli, Wojciech Galuba, Florian Metze, and Christoph Feichtenhofer. Masked autoencoders that listen. *Advances in Neural Information Processing Systems*, 35:28708–28720, 2022. [20](#)

[40] Po-Yao Huang, Vasu Sharma, Hu Xu, Chaitanya Ryali, haoqi fan, Yanghao Li, Shang-Wen Li, Gargi Ghosh, Jitendra Malik, and Christoph Feichtenhofer. Mavil: Masked audio-video learners. In *Advances in Neural Information Processing Systems*, pages 20371–20393. Curran Associates, Inc., 2023. [21](#)

[41] Hyeonuk Nam and Seong-Hu Kim and Byeong-Yun Ko and Yong-Hwa Park. Frequency Dynamic Convolution: Frequency-Adaptive Pattern Recognition for Sound Event Detection. In *Interspeech 2022*, pages 2763–2767, 2022. [21](#)

[42] Gabriel Ilharco, Mitchell Wortsman, Ross Wightman, Cade Gordon, Nicholas Carlini, Rohan Taori, Achal Dave, Vaishaal Shankar, Hongseok Namkoong, John Miller, Hannaneh Hajishirzi, Ali Farhadi, and Ludwig Schmidt. OpenCLIP, 2021. [20](#)

[43] Chao Jia, Yinfei Yang, Ye Xia, Yi-Ting Chen, Zarana Parekh, Hieu Pham, Quoc Le, Yun-Hsuan Sung, Zhen Li, and Tom Duerig. Scaling up visual and vision-language representation learning with noisy text supervision. In *ICML*, 2021. [20](#)

[44] Cijo Jose, Théo Moutakanni, Dahyun Kang, Federico Baldassarre, Timothée Darcet, Hu Xu, Daniel Li, Marc Szafraniec, Michaël Ramamonjisoa, Maxime Oquab, Oriane Siméoni, Huy V. Vo, Patrick Labatut, and Piotr Bojanowski. DINOv2 meets text: A unified framework for image- and pixel-level vision-language alignment. In *CVPR*, 2025. 20

[45] Will Kay, Joao Carreira, Karen Simonyan, Brian Zhang, Chloe Hillier, Sudheendra Vijayanarasimhan, Fabio Viola, Tim Green, Trevor Back, Paul Natsev, Mustafa Suleyman, and Andrew Zisserman. The kinetics human action video dataset. *arXiv:1705.06950*, 2017. 10, 12, 28

[46] Chris Dongjoo Kim, Byeongchang Kim, Hyunmin Lee, and Gunhee Kim. Audiocaps: Generating captions for audios in the wild. In *Proceedings of the 2019 Conference of the North American Chapter of the Association for Computational Linguistics: Human Language Technologies, Volume 1 (Long and Short Papers)*, pages 119–132, 2019. 10, 11, 12, 25, 28

[47] Jaeyeon Kim, Jaeyoon Jung, Jinjoo Lee, and Sang Hoon Woo. Enclap: Combining neural audio codec and audio-text joint embedding for automated audio captioning. *arXiv preprint arXiv:2401.17690*, 2024. 4, 10, 13, 21, 28

[48] Hildegard Kuehne, Hueihan Jhuang, Estíbaliz Garrote, Tomaso Poggio, and Thomas Serre. HMDB: a large video database for human motion recognition. In *ICCV*, 2011. 10, 12

[49] Étienne Labb  , Thomas Pellegrini, and Julien Pinquier. Conete: An efficient audio captioning system leveraging multiple datasets with task embedding, 2023. 4, 13, 21, 28

[50] Zhengfeng Lai, Haotian Zhang, Bowen Zhang, Wentao Wu, Haoping Bai, Aleksei Timofeev, Xianzhi Du, Zhe Gan, Jiulong Shan, Chen-Nee Chuah, Yinfei Yang, and Meng Cao. VeCLIP: Improving CLIP training via visual-enriched captions. In *ECCV*, 2024. 20

[51] Kunchang Li, Yali Wang, Yizhuo Li, Yi Wang, Yinan He, Limin Wang, and Yu Qiao. Unmasked teacher: Towards training-efficient video foundation models. In *ICCV*, 2023. 12

[52] Xianhang Li, Zeyu Wang, and Cihang Xie. CLIPA-v2: Scaling CLIP training with 81.1% zero-shot imagenet accuracy within a \$10,000 budget; an extra \$4,000 unlocks 81.8% accuracy. *arXiv:2306.15658*, 2023. 20

[53] Xian Li, Nian Shao, and Xiaofei Li. Self-supervised audio teacher-student transformer for both clip-level and frame-level tasks. *IEEE/ACM Transactions on Audio, Speech, and Language Processing*, 32:1336–1351, 2024. 17, 21

[54] Yanghao Li, Haoqi Fan, Ronghang Hu, Christoph Feichtenhofer, and Kaiming He. Scaling language-image pre-training via masking. In *CVPR*, 2023. 20

[55] Yizhi Li, Ruibin Yuan, Ge Zhang, Yinghao Ma, Xingran Chen, Hanzhi Yin, Chenghao Xiao, Chenghua Lin, Anton Ragni, Emmanouil Benetos, et al. Mert: Acoustic music understanding model with large-scale self-supervised training. In *International Conference on Learning Representations*, 2024. 20

[56] Alexander H Liu, Heng-Jui Chang, Michael Auli, Wei-Ning Hsu, and Jim Glass. Dinosr: Self-distillation and online clustering for self-supervised speech representation learning. In *Advances in Neural Information Processing Systems*, pages 58346–58362, 2023. 20

[57] Haotian Liu, Chunyuan Li, Qingyang Wu, and Yong Jae Lee. Visual instruction tuning. *NeurIPS*, 2024. 20

[58] AI @ Meta Llama Team. The llama 3 herd of models. *arXiv:2407.21783*, 2024. 4

[59] Harry McGurk and John MacDonald. Hearing lips and seeing voices. *Nature*, 264:746–748, 1976. 1

[60] Brandon McKinzie, Zhe Gan, Jean-Philippe Fauconnier, Sam Dodge, Bowen Zhang, Philipp Duffer, Dhruti Shah, Xianzhi Du, Futang Peng, Floris Weers, Anton Belyi, Haotian Zhang, Karanjeet Singh, Doug Kang, Ankur Jain, Hongyu H  , Max Schwarzer, Tom Gunter, Xiang Kong, Aonan Zhang, Jianyu Wang, Chong Wang, Nan Du, Tao Lei, Sam Wiseman, Guoli Yin, Mark Lee, Zirui Wang, Ruoming Pang, Peter Grasch, Alexander Toshev, and Yinfei Yang. MM1: methods, analysis and insights from multimodal LLM pre-training. In *ECCV*, 2024. 20

[61] Annamaria Mesaros, Toni Heittola, and Tuomas Virtanen. Metrics for polyphonic sound event detection. *Applied Sciences*, 6(6):162, 2016. 17

[62] Annamaria Mesaros, Toni Heittola, Tuomas Virtanen, and Mark D Plumley. Sound event detection: A tutorial. *IEEE Signal Processing Magazine*, 38(5):67–83, 2021. 21

[63] Norman Mu, Alexander Kirillov, David Wagner, and Saining Xie. SLIP: Self-supervision meets language-image pre-training. In *ECCV*, 2022. 20

[64] Muhammad Ferjad Naeem, Yongqin Xian, Xiaohua Zhai, Lukas Hoyer, Luc Van Gool, and Federico Tombari. SILC: Improving vision language pretraining with self-distillation. In *ECCV*, 2024. 20

[65] Thao Nguyen, Samir Yitzhak Gadre, Gabriel Ilharco, Sewoong Oh, and Ludwig Schmidt. Improving multimodal datasets with image captioning. In *NeurIPS*, 2023. 20

[66] Tu Anh Nguyen, Wei-Ning Hsu, Antony d’Avirro, Bowen Shi, Itai Gat, Maryam Fazel-Zarani, Tal Remez, Jade Copet, Gabriel Synnaeve, Michael Hassid, et al. Expresso: A benchmark and analysis of discrete expressive speech resynthesis. *arXiv preprint arXiv:2308.05725*, 2023. 11

[67] Daisuke Niizumi, Daiki Takeuchi, Yasunori Ohishi, Noboru Harada, Masahiro Yasuda, Shunsuke Tsubaki, and Keisuke Imoto. M2D-CLAP: Masked Modeling Duo Meets CLAP for Learning General-purpose Audio-Language Representation. *to appear at Interspeech*, 2024. 2, 10, 11, 20, 30

[68] Maxime Oquab, Timothée Darcet, Théo Moutakanni, Huy Vo, Marc Szafraniec, Vasil Khalidov, Pierre Fernandez, Daniel Haziza, Francisco Massa, Alaaeldin El-Nouby, Mahmoud Assran, Nicolas Ballas, Wojciech Galuba, Russell Howes, Po-Yao Huang, Shang-Wen Li, Ishan Misra, Michael Rabbat, Vasu Sharma, Gabriel Synnaeve, Hu Xu, Hervé Jégou, Julien Mairal, Patrick Labatut, Armand Joulin, and Piotr Bojanowski. Dinov2: Learning robust visual features without supervision, 2023. 8

[69] Zhiliang Peng, Wenhui Wang, Li Dong, Yaru Hao, Shaohan Huang, Shuming Ma, and Furu Wei. Kosmos-2: Grounding multimodal large language models to the world. *arXiv:2306.14824*, 2023. 20

[70] Karol J. Piczak. Esc: Dataset for environmental sound classification. In *Proceedings of the 23rd ACM International Conference on Multimedia (ACM MM)*, pages 1015–1018, 2015. 10, 11

[71] Adam Polyak, Amit Zohar, Andrew Brown, Andros Tjandra, Animesh Sinha, Ann Lee, Apoorv Vyas, Bowen Shi, Chih-Yao Ma, Ching-Yao Chuang, David Yan, Dhruv Choudhary, Dingkang Wang, Geet Sethi, Guan Pang, Haoyu Ma, Ishan Misra, Ji Hou, Jialiang Wang, Kiran Jagadeesh, Kunpeng Li, Luxin Zhang, Mannat Singh, Mary Williamson, Matt Le, Matthew Yu, Mitesh Kumar Singh, Peizhao Zhang, Peter Vajda, Quentin Duval, Rohit Girdhar, Roshan Sumbaly, Sai Saketh Rambhatla, Sam Tsai, Samaneh Azadi, Samyak Datta, Sanyuan Chen, Sean Bell, Sharadh Ramaswamy, Shelly Sheynin, Siddharth Bhattacharya, Simran Motwani, Tao Xu, Tianhe Li, Tingbo Hou, Wei-Ning Hsu, Xi Yin, Xiaoliang Dai, Yaniv Taigman, Yaqiao Luo, Yen-Cheng Liu, Yi-Chiao Wu, Yue Zhao, Yuval Kirstain, Zecheng He, Zijian He, Albert Pumarola, Ali Thabet, Artsiom Sanakoyeu, Arun Mallya, Baishan Guo, Boris Araya, Breena Kerr, Carleigh Wood, Ce Liu, Cen Peng, Dmitry Vengertsev, Edgar Schonfeld, Elliot Blanchard, Felix Juefei-Xu, Fraylie Nord, Jeff Liang, John Hoffman, Jonas Kohler, Kaolin Fire, Karthik Sivakumar, Lawrence Chen, Licheng Yu, Luya Gao, Markos Georgopoulos, Rashel Moritz, Sara K. Sampson, Shikai Li, Simone Parmeggiani, Steve Fine, Tara Fowler, Vladan Petrovic, and Yuming Du. Movie gen: A cast of media foundation models. *arXiv preprint arXiv:2410.13720*, 2024. 5, 17

[72] Vineel Pratap, Andros Tjandra, Bowen Shi, Paden Tomasello, Arun Babu, Sayani Kundu, Ali Elkahky, Zhaocheng Ni, Apoorv Vyas, Maryam Fazel-Zarandi, et al. Scaling speech technology to 1,000+ languages. *Journal of Machine Learning Research*, 25(97):1–52, 2024. 4

[73] Alec Radford, Jong Wook Kim, Chris Hallacy, Aditya Ramesh, Gabriel Goh, Sandhini Agarwal, Girish Sastry, Amanda Askell, Pamela Mishkin, Jack Clark, Gretchen Krueger, and Ilya Sutskever. Learning transferable visual models from natural language supervision. In *ICML*, 2021. 1, 8, 20

[74] Alec Radford, Jong Wook Kim, Tao Xu, Greg Brockman, Christine McLeavey, and Ilya Sutskever. Robust speech recognition via large-scale weak supervision, 2022. 4

[75] Justin Salamon, Christopher Jacoby, and Juan Pablo Bello. A dataset and taxonomy for urban sound research. In *Proceedings of the 22nd ACM International Conference on Multimedia (ACM MM)*, pages 1041–1044, Orlando, FL, USA, 2014. 10, 11

[76] Justin Salamon, Duncan MacConnell, Mark Cartwright, Peter Li, and Juan Pablo Bello. Scaper: A library for soundscape synthesis and augmentation. In *WASPAA*, pages 344–348, 2017. 17

[77] Mert Bulent Sarayildiz, Julien Perez, and Diane Larlus. Learning visual representations with caption annotations. In *ECCV*, 2020. 20

[78] Florian Schmid, Tobias Morocutti, Francesco Foscarin, Jan Schlüter, Paul Primus, and Gerhard Widmer. Effective

pre-training of audio transformers for sound event detection. In *IEEE International Conference on Acoustics, Speech and Signal Processing (ICASSP)*, 2025. 17, 18, 21

[79] Christoph Schuhmann, Romain Beaumont, Richard Vencu, Cade W Gordon, Ross Wightman, Mehdi Cherti, Theo Coombes, Aarush Katta, Clayton Mullis, Mitchell Wortsman, Patrick Schramowski, Srivatsa R Kundurthy, Katherine Crowson, Ludwig Schmidt, Robert Kaczmarczyk, and Jenia Jitsev. LAION-5b: An open large-scale dataset for training next generation image-text models. In *NeurIPS Datasets and Benchmarks*, 2022. 20

[80] Nian Shao, Xian Li, and Xiaofei Li. Fine-tune the pretrained atst model for sound event detection. In *ICASSP 2024-2024 IEEE International Conference on Acoustics, Speech and Signal Processing (ICASSP)*, pages 911–915. IEEE, 2024. 21

[81] Bowen Shi, Andros Tjandra, John Hoffman, Helin Wang, Yi-Chiao Wu, Luya Gao, Julius Richter, Matt Le, Apoorv Vyas, Sanyuan Chen, Christoph Feichtenhofer, Piotr Dollár, Wei-Ning Hsu, and Ann Lee. Sam-audio: Segment anything in audio. 2025.

[82] Khurram Soomro, Amir Roshan Zamir, and Mubarak Shah. UCF101: A dataset of 101 human actions classes from videos in the wild. *arXiv:1212.0402*, 2012. 12

[83] Jianlin Su, Yu Lu, Shengfeng Pan, Bo Wen, and Yunfeng Liu. RoFormer: Enhanced transformer with rotary position embedding. *Neurocomputing*, 2024. 6, 26

[84] Quan Sun, Yuxin Fang, Ledell Wu, Xinlong Wang, and Yue Cao. EVA-CLIP: Improved training techniques for clip at scale. *arXiv:2303.15389*, 2023. 20

[85] Shengbang Tong, Ellis Brown, Penghao Wu, Sanghyun Woo, Manoj Middepogu, Sai Charitha Akula, Jihan Yang, Shusheng Yang, Adithya Iyer, Xichen Pan, Ziteng Wang, Rob Fergus, Yann LeCun, and Saining Xie. Cambrian-1: A fully open, vision-centric exploration of multimodal llms. In *NeurIPS*, 2024. 20

[86] Michael Tschannen, Manoj Kumar, Andreas Steiner, Xiaohua Zhai, Neil Houlsby, and Lucas Beyer. Image captioners are scalable vision learners too. In *NeurIPS*, 2023. 20

[87] Michael Tschannen, Alexey Gritsenko, Xiao Wang, Muhammad Ferjad Naeem, Ibrahim Alabdulmohsin, Nikhil Parthasarathy, Talfan Evans, Lucas Beyer, Ye Xia, Basil Mustafa, Olivier Hénaff, Jeremiah Harmsen, Andreas Steiner, and Xiaohua Zhai. SigLIP 2: Multilingual vision-language encoders with improved semantic understanding, localization, and dense features. *arXiv:2502.14786*, 2025. 11, 12

[88] Nicolas Turpault, Romain Serizel, Ankit Shah, and Justin Salamon. DESED_public_eval. <https://doi.org/10.5281/zenodo.3588172>, 2019. Dataset. Creative Commons Attribution 4.0 International (CC-BY 4.0). 17

[89] Nicolas Turpault, Romain Serizel, Ankit Parag Shah, and Justin Salamon. Sound event detection in domestic environments with weakly labeled data and soundscape synthesis. In *Workshop on Detection and Classification of Acoustic Scenes and Events*, 2019. 3, 17, 18, 21

[90] George Tzanetakis and Perry Cook. Musical genre classification of audio signals. *IEEE Transactions on Speech and Audio Processing*, 10(5):293–302, 2002. 10, 11

[91] Apoorv Vyas, Bowen Shi, Matthew Le, Andros Tjandra, Yi-Chiao Wu, Baishan Guo, Jiemin Zhang, Xinyue Zhang, Robert Adkins, William Ngan, Jeff Wang, Ivan Cruz, Bapi Akula, Akinniyi Akinyemi, Brian Ellis, Rashel Moritz, Yael Yungster, Alice Rakotoarison, Liang Tan, Chris Summers, Carleigh Wood, Joshua Lane, Mary Williamson, and Wei-Ning Hsu. Audiobox: Unified audio generation with natural language prompts, 2023. 4

[92] Bo Wan, Michael Tschannen, Yongqin Xian, Filip Pavetic, Ibrahim M Alabdulmohsin, Xiao Wang, André Susano Pinto, Andreas Steiner, Lucas Beyer, and Xiaohua Zhai. LocCa: Visual pretraining with location-aware captioners. In *NeurIPS*, 2024. 20

[93] Xin Wang, Jiawei Wu, Junkun Chen, Lei Li, Yuan-Fang Wang, and William Yang Wang. Vatex: A large-scale, high-quality multilingual dataset for video-and-language research. In *Proceedings of the IEEE/CVF international conference on computer vision*, pages 4581–4591, 2019. 12

[94] Yi Wang, Kunchang Li, Xinhao Li, Jiashuo Yu, Yinan He, Guo Chen, Baoqi Pei, Rongkun Zheng, Zun Wang, Yansong Shi, Tianxiang Jiang, Songze Li, Jilan Xu, Hongjie Zhang, Yifei Huang, Yu Qiao, Yali Wang, and Limin Wang. InternVideo2: Scaling foundation models for multimodal video understanding. In *ECCV*, 2024. 1, 2, 11, 12, 20, 21

[95] Benjamin Warner, Antoine Chaffin, Benjamin Clavié, Orion Weller, Oskar Hallström, Said Taghadouini, Alexis Gallagher, Raja Biswas, Faisal Ladhak, Tom Aarsen, Nathan Cooper, Griffin Adams, Jeremy Howard, and

Iacopo Poli. Smarter, better, faster, longer: A modern bidirectional encoder for fast, memory efficient, and long context finetuning and inference. In *Proceedings of the 63rd Annual Meeting of the Association for Computational Linguistics (ACL), Long Papers*, Vienna, Austria, 2025. 5, 17, 28

[96] Yusong Wu*, Ke Chen*, Tianyu Zhang*, Yuchen Hui*, Taylor Berg-Kirkpatrick, and Shlomo Dubnov. Large-scale contrastive language-audio pretraining with feature fusion and keyword-to-caption augmentation. In *IEEE International Conference on Acoustics, Speech and Signal Processing, ICASSP*, 2023. 1, 2, 10, 11, 20, 25, 30

[97] Yusong Wu, Christos Tsirigotis, Ke Chen, Cheng-Zhi Anna Huang, Aaron Courville, Oriol Nieto, Prem Seetharaman, and Justin Salamon. SED-augmented adobe audition sound effects dataset (ASFX-SED). <https://doi.org/10.5281/zenodo.15866339>, 2025. Dataset. Adobe Research License. 17

[98] Yusong Wu, Christos Tsirigotis, Ke Chen, Cheng-Zhi Anna Huang, Aaron Courville, Oriol Nieto, Prem Seetharaman, and Justin Salamon. FLAM: Frame-wise language-audio modeling. In *ICML*, 2025. 17, 18, 21

[99] Hu Xu, Po-Yao Huang, Xiaoqing Ellen Tan, Ching-Feng Yeh, Jacob Kahn, Christine Jou, Gargi Ghosh, Omer Levy, Luke Zettlemoyer, Wen tau Yih, Shang-Wen Li, Saining Xie, and Christoph Feichtenhofer. Altogether: Image captioning via re-aligning alt-text. In *EMNLP*, 2024. 20

[100] Hu Xu, Saining Xie, Xiaoqing Ellen Tan, Po-Yao Huang, Russell Howes, Vasu Sharma, Shang-Wen Li, Gargi Ghosh, Luke Zettlemoyer, and Christoph Feichtenhofer. Demystifying clip data. In *ICLR*, 2024. 1, 8, 20

[101] Jun Xu, Tao Mei, Ting Yao, and Yong Rui. MSR-VTT: A large video description dataset for bridging video and language. In *CVPR*, 2016. 10, 12, 20, 28

[102] Jin Xu, Zhifang Guo, Hangrui Hu, Yunfei Chu, Xiong Wang, Jinzheng He, Yuxuan Wang, Xian Shi, Ting He, Xinfu Zhu, Yuanjun Lv, Yongqi Wang, Dake Guo, He Wang, Linhan Ma, Pei Zhang, Xinyu Zhang, Hongkun Hao, Zishan Guo, Baosong Yang, Bin Zhang, Ziyang Ma, Xipin Wei, Shuai Bai, Keqin Chen, Xuejing Liu, Peng Wang, Mingkun Yang, Dayiheng Liu, Xingzhang Ren, Bo Zheng, Rui Men, Fan Zhou, Bowen Yu, Jianxin Yang, Le Yu, Jingren Zhou, and Junyang Lin. Qwen3-omni technical report. *arXiv preprint arXiv:2509.17765*, 2025. 20

[103] Junichi Yamagishi, Christophe Veaux, and Kirsten MacDonald. Cstr vctk corpus: English multi-speaker corpus for cstr voice cloning toolkit. In *Proc. IEEE International Conference on Acoustics, Speech and Signal Processing (ICASSP)*, 2019. 10, 11

[104] Zhenhui Ye, Rongjie Huang, Yi Ren, Ziyue Jiang, Jinglin Liu, Jinzheng He, Xiang Yin, and Zhou Zhao. CLAPSpeech: Learning prosody from text context with contrastive language-audio pre-training. In *Proceedings of the 61st Annual Meeting of the Association for Computational Linguistics (Volume 1: Long Papers)*, pages 9317–9331, Toronto, Canada, 2023. Association for Computational Linguistics. 1, 10

[105] Ching-Feng Yeh, Po-Yao Huang, Vasu Sharma, Shang-Wen Li, and Gargi Gosh. Flap: Fast language-audio pre-training. In *2023 IEEE Automatic Speech Recognition and Understanding Workshop (ASRU)*, pages 1–8, 2023. 20

[106] Jiahui Yu, Zirui Wang, Vijay Vasudevan, Legg Yeung, Mojtaba Seyedhosseini, and Yonghui Wu. CoCa: Contrastive captioners are image-text foundation models. *TMLR*, 2022. 20

[107] Chien Yu Huang, Wei-Chih Chen, Shu-wen Yang, Andy T. Liu, Chen-An Li, Yu-Xiang Lin, Wei-Cheng Tseng, Anuj Diwan, Yi-Jen Shih, Jiatong Shi, William Chen, Chih-Kai Yang, Wenze Ren, Xuanjun Chen, Chi-Yuan Hsiao, Puyuan Peng, Shih-Heng Wang, Chun-Yi Kuan, Ke-Han Lu, Kai-Wei Chang, Fabian Ritter-Gutierrez, Kuan-Po Huang, Siddhant Arora, You-Kuan Lin, Ming To Chuang, Eunjung Yeo, Kelvin Chang, Chung-Ming Chien, Kwanghee Choi, Jun-You Wang, Cheng-Hsiu Hsieh, Yi-Cheng Lin, Chee-En Yu, I-Hsiang Chiu, Heitor R. Guimaraes, Jionghao Han, Tzu-Quan Lin, Tzu-Yuan Lin, Homu Chang, Ting-Wu Chang, Chun Wei Chen, Shou-Jen Chen, Yu-Hua Chen, Hsi-Chun Cheng, Kunal Dhawan, Jia-Lin Fang, Shi-Xin Fang, Kuan-Yu Fang Chiang, Chi An Fu, Hsien-Fu Hsiao, Ching Yu Hsu, Shao-Syuan Huang, Lee Chen Wei, Hsi-Che Lin, Hsuan-Hao Lin, Hsuan-Ting Lin, Jian-Ren Lin, Ting-Chun Liu, Li-Chun Lu, Tsung-Min Pai, Ankita Pasad, Shih-Yun Shan Kuan, Suwon Shon, Yuxun Tang, Yun-Shao Tsai, Jui-Chiang Wei, Tzu-Chieh Wei, Chengxi Wu, Dien-Ruei Wu, Chao-Han Huck Yang, Chieh-Chi Yang, Jia Qi Yip, Shao-Xiang Yuan, Vahid Noroozi, Zhehuai Chen, Haibin Wu, Karen Livescu, David Harwath, Shinji Watanabe, and Hung yi Lee. Dynamic-superb phase-2: A collaboratively expanding benchmark for measuring the capabilities of spoken language models with 180 tasks, 2025. 10, 11, 28

[108] Xiaohua Zhai, Basil Mustafa, Alexander Kolesnikov, and Lucas Beyer. Sigmoid loss for language image pre-training. In *ICCV*, 2023. 7, 8, 20

[109] Yuhao Zhang, Hang Jiang, Yasuhide Miura, Christopher D. Manning, and Curtis P. Langlotz. Contrastive learning of medical visual representations from paired images and text. In *MLHC*, 2022. 20

- [110] Long Zhao, Nitesh Bharadwaj Gundavarapu, Liangzhe Yuan, Hao Zhou, Shen Yan, Jennifer J. Sun, Luke Friedman, Rui Qian, Tobias Weyand, Yue Zhao, Rachel Hornung, Florian Schroff, Ming Yang, David A. Ross, Huisheng Wang, Hartwig Adam, Mikhail Sirotenko, Ting Liu, and Boqing Gong. VideoPrism: A foundational visual encoder for video understanding. In *ICML*, 2024. [11](#)
- [111] Bin Zhu, Bin Lin, Munan Ning, Yang Yan, Jiaxi Cui, Wang HongFa, Yatian Pang, Wenhao Jiang, Junwu Zhang, Zongwei Li, Cai Wan Zhang, Zhifeng Li, Wei Liu, and Li Yuan. Languagebind: Extending video-language pretraining to n-modality by language-based semantic alignment, 2023. [1](#), [2](#), [10](#), [11](#), [12](#), [21](#), [30](#), [31](#)
- [112] Haina Zhu, Yizhi Zhou, Hangting Chen, Jianwei Yu, Ziyang Ma, Rongzhi Gu, Yi Luo, Wei Tan, and Xie Chen. Muq: Self-supervised music representation learning with mel residual vector quantization. *arXiv preprint arXiv:2501.01108*, 2025. [20](#)